Novel sol-immobilization catalysts for the hydrogenation of levulinic acid and spectroscopic evaluation of metal nanoparticles accessibility using probe molecules.

Thesis submitted for the title of MPhil

Candidate: Giacomo Marco Lari

ID number: 1236332

2014

Summary

Hydrogenation of levulinic acid to gamma-valerolactone has been studied with novel supported-ruthenium catalyst, achieving high conversion and selectivity in mild condition and using water as a green solvent. Sol immobilization has been applied successfully with the aim of increasing the turnover of the hydrogenation reaction per atom of ruthenium. This allows the preparation of supported metal catalysts with lower loading (1 wt.%) in comparison with the established commercial standard (5 wt.%). The study of the influence of the ruthenium precursor has been performed and the results obtained with the best catalyst have been compared with those obtained with different preparation methods. The catalysts were characterized through nitrogen sorption, temperature programmed reduction, CO chemisorption and X-ray diffraction to determine the structure and properties of the support and of the active phase and to make hypotheses regarding the structure-activity relationship. Reusability tests were performed to asses the industrial validity of this system, the result showing that though high performances are achieved with fresh catalysts, deactivation issues have still to be addressed.

A deeper investigation of sol-immobilization catalysts and in particular of the role of the capping agent used in the preparation of the metal sol has been performed using titania-supported gold catalysts. The adsorption of carbon monoxide was monitored by the use of infrared and UV-vis spectroscopy on 1 wt.% Au/TiO_2 prepared by sol immobilization using polyvinylalcohol and polyvinylpyrrolidone as stabilisers before and after treatments to remove the polymer from the surface. Comparison of spectroscopic results obtained on these catalysts with accessible deposition-precipitation-prepared catalyst allowed finding a relationship between the activity of the catalyst in CO oxidation and the accessibility of the surface. These newly developed tools allow for a easier characterization of the metal surface of supported gold catalysts.

Table of Contents

1. Novel sol-immobilization catalysts for the hydrogenation of levulinic acid

1.1. Introduction

Government all around the world are stimulating the exploitation of renewable energies and resources. This is driven by some main factors; the biggest part of the fossil fuel reserves is located in few countries and it is in the interest of a nation to have access to its own energy source. Moreover, some predictions claim that fossil resources will not be able to satisfy the world's energy needs by 2050. Secondly, it is important to find CO_2 neutral sources, in order to contrast the threat of climate changes. Some nations push towards biomasses exploitation also to develop and improve agricultural activities.[1]

Nowadays the fossil fuel exploitation is split with about three quarter for heat and power generation, one quarter for transportation and a few per cent for chemicals. Green alternatives are already possible for the heat and power generation, namely hydropower, wind, solar and biomasses. It is instead more difficult to replace transportation fuel with renewable and CO_2 neutral substance, as it must meet strict specification. The first generation of biofuels that can be already found on the market is represented by sugar, starch and oil-derivatives. While it contributed slightly to the growth of the market and to a stabilization of the fuel's price, it is not a viable strategy on the long term. In fact it competes with food for fertile grounds, and it does not have a great efficiency when the power consumption for growing the crops is taken into account. Some authors report that 60-75 % of the bioethanol energy is used for growing and processing crops.[2-4]

The ways of overcoming this could be found in the exploitation of crop residues for the production of chemicals and fuels. This are called lignocellulosic materials, as are made of cellulose, hemicellulose and lignin, apart from water.

Cellulose represents the 40 % of these materials. It is a high molecular weight polymer of glucose, whose chains are held together as fibres, conferring strength to the material. The hemicellulose accounts for the 25 % of the weight and is the low molecular weight polymer of glucose; it holds the cellulose chains together. Both these polymers are attractive as a source of glucose, once physical treatment and depolymerisation are achieved. Lignin, accounting for the 20 %, is a propyl-phenol tri-dimensional polymer, bound to the hemicellulose, which gives rigidity to the structure. Recent studies for its valorisation suggest upgrading to dispersants and other high added-value chemicals. Fatty acids, terpenic oils and inorganic materials represent the rest of the weight.

The challenge in the conversion of lignocellulose is opposite to that represented in the processing of crude oil. While the former is mostly constituted by aliphatic hydrocarbon, and thus lacks of any functional group, the former has an excessive presence of functionalities. The success in the conversion of lignocellulose to value-added products will give the chemical and the fuel industry an alternative feedstock for their activities that could prove to be useful in different economic conditions.

In order to obtain fuels and chemicals, lignocellulose has to be deoxygenated, after it has been depolymerized. Fuels require low oxygenated molecules; because oxygen usually lowers the heat content of the compound ($\Delta H_{\text{combustion, glucose}}$ = 2.8 kJ/mol, *vs.* $\Delta H_{\text{comb, hexane}}$ = 4.1 kJ/mol), while chemicals require a selected mix of functional groups.

The simplest method to achieve these is pyrolysis, leading to charcoal and fuel gas. The former is light and porous and has a high-energy content (30 GJ/ton), while the latter has lower energy content and could be used for energy and heat generation.[1] Another important process is gasification; the syngas ($CO+H_2$) obtained could be used for the production of paraffin (Fischer-Tropsch process), methanol and olefins (Methanol to olefins). Both these two processes use extreme temperature conditions to convert lignocellulosic feedstock.[5,6]

Conversion to more valuable products can be achieved also milder conditions exploiting the reactivity of the functional groups present. Depolymerisation to the sugars is easily accomplished at relatively low temperature (<200 °C) in the presence of an acid or basic catalyst. The amount of by-products depends on the reaction conditions; these are formed by acid or base-catalysed decomposition and dehydration reactions. Amongst the by-products there are furan species (furfural and hydroxymethylfurfural, HMF), levulinic acid (LA) and formic acid.[7-9] Deoxigenation of the resulting hydrolysis product could be achieved through dehydration (through the removal of water from the molecule) or through hydrogenation or hydrogenolysis.

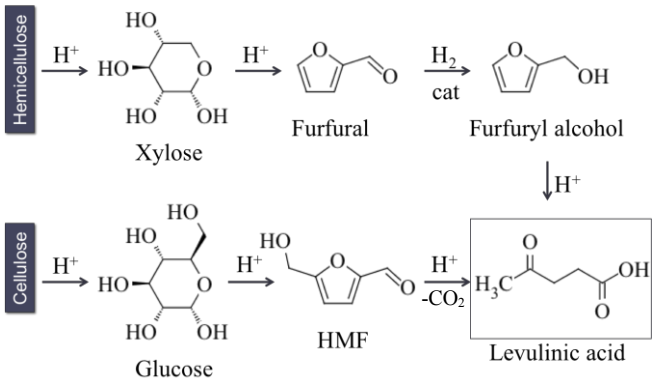

Figure 1: cellulose and hemicellulose pathways to LA

Amongst all the products formed in these reactions as a function of their conditions, it has been predicted that levulinic acid (Figure 1) will play an important role in the near future in the substitution of petro chemistry based with renewable sugar based synthetic routes.[10] In particular, through the hydrogenation of the carbonyl group, followed by cyclization, levulinic acid (LA) could be transformed into γ-valerolactone (GVL, Figure 2). The physico-chemical properties of GVL have been discussed by Horvat et al. and it proved to be a promising biofuels that can be mixed at 10 v/v % with gasoline to be used in common engines.[11] Furthermore it is used as an industrial solvent and is a precursor for polyesters.

LA hydrogenation to γ-valerolactone

Introduction

The hydrogenation of LA to GVL is a two step reaction that could involve two different pathways (Figure 2).

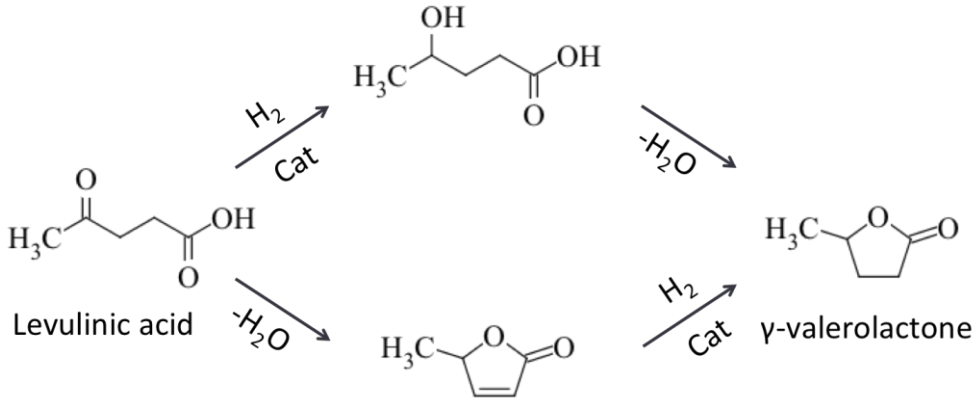

Figure 2: LA conversion to GVL, two different reaction pathways.

The two different paths involve significantly different steps. In the first case the carbonyl function is hydrogenated to a secondary alcohol, leading to 4-hydroxyvaleric acid. This compound is not stable and spontaneously cyclize to the lactone. In the equilibrium the lactone is favoured, and the rate is mostly influenced by the presence of acid catalysts and temperature. This first route is favoured at low temperature and in the presence of a catalyst that hydrogenates preferentially the carbonyl.

The second pathway is favoured at high temperature, where the formation of the enol form of LA and its subsequent cyclization to the unsaturated lactone (α or β-angelica lactone) is favoured. This compound is then hydrogenated to GVL and thus requires a catalyst that is able to add a hydrogen molecule to a C=C double bond.

Generally, the first route is preferred.

First catalytic attempts

First experiments regarding the reduction of levulinic acid to γ-hydroxyvaleric acid and the corresponding γ-valerolactone were performed in the second half of the nineteenth century. Wollf performed this reaction using a sodium amalgam as the reducing agent in 1881.[12] At the beginning of the 20th century Losanitsch and Schütte used metallic sodium in ethanol, achieving 60 % yield.[13,14] All these experiments used stoichiometric agents, resulting in low atom economy processes. Sabatier performed the first catalytic experiments using molecular hydrogen at the beginning of the 20th century, working at 250 °C in vapour phase and in the presence of a nickel catalyst.[15] Schuette et al. performed a similar reaction at room temperature, in ethyl ether, in the presence of a platinum oxide catalyst under a 3 atmosphere hydrogen pressure.[16] They claimed 87 % selectivity and 90 % conversion after two days. Even though the reaction does not go to completion and takes a long time the paper describes for the first time the possibility of hydrogenating levulinic acid in liquid phase. The influence of three solvents (acetic acid, ethanol and diethyl ether) is shown and the better yields achieved with the ether could be attributed to the better solubility of hydrogen in this solvent.[17] It has been also shown that an alcoholic solvent is not indicated, because it leads to the formation of the ester. The use of a low-boiling point solvent, such as the diethyl ether, eases the product separation.

Since then almost all the published reactions for the hydrogenation of levulinic acid to γ-valerolactone are catalytic, involving the use of molecular hydrogen and of a catalyst. In the 1940s Kyrides et al. patented a process where levulinic acid was hydrogenated at high temperature and pressure (200 °C, 60 atm) in the presence of a nickel Raney catalyst.[18] The process achieved high yield (92 %) in relatively short time (4,5 hours). The same methodology has been used in other papers due to its simplicity, especially in terms of catalyst preparation, as sponge metal catalysts are available commercially and produced easily.[19] In this process the levulinic acid was used as a water solution. Water is considered a green solvent; it is not toxic and not polluting. Nevertheless it is not always preferred in an industrial process, because of

its relatively high boiling point and the high energy and plant requirements for a good separation, particularly from polar molecules as acids, alcohols and esters.

Copper chromite

The effectiveness of noble metals in the hydrogenation is known since a long time. Unfortunately they are usually very expensive and for this reason the industry has adopted processes based upon them only once problems as deactivation, catalyst recovery and metal leaching were solved.

A patent filed in 1953 describes a process that for the first time does not involve one of those metals, using instead a copper chromite catalyst.[20] The reaction is performed at high temperature (200 °C) in vapour phase at atmospheric pressure with selectivity and conversion close to 100 %. The major disadvantage of operating in gas phase and very low pressure on the industrial scale is that the dimensions of the plant are bigger, leading to an increase in the plant's price. Copper chromite was firstly described by Gröger in 1908 and has composition $Cu_2Cr_2O_5$.[21,22] Since then they have been used for hydrogenation of organic molecules. They are particularly active towards carbonyl groups of aldehyde, ketones and ester but also towards pyrroles, indoles and carbazoles and were extensively studied since the first half of the last century in terms of catalytic activity, structure and synthesis.[23-30] Adkins studied the activity in the hydrogenation of many carbonyl groups in the liquid phase, working with a very high hydrogen pressure (100-150 bar) but demonstrating that the already noted hydrogenating activity in the gas phase was kept also in the liquid.[23]

Noble metals

Noble metals in their supported forms have been widely investigated in terms of their activity in the levulinic acid hydrogenation reaction. It is possible to find many experimental data about platinum, iridium, rhenium, palladium, ruthenium and gold.

Nevertheless the most studied systems are those employing rhenium or ruthenium catalyst. They both show an outstanding hydrogenating activity, along with high selectivity to the carbonyl group. The next paragraphs deal with these two catalysts.

Rhenium catalysts

In 1959 Broadbent's work showed the feasibility of the levulinic acid hydrogenation reaction in liquid phase and without solvent using rhenium black, i.e. metallic rhenium powder, obtained reducing the oxide in situ.[31] The yields are not elevated (71 %) though the pressure and the reaction times are high. Nevertheless the work showed the possibility of working in liquid phase without solvent, which results in smaller plant size. Surprisingly, the catalyst does not hydrogenate the carboxylic functional group of the levulinic acid, nor the lactone carbonyl while it showed a good activity towards hydrogenation of, for example, acetic acid to ethanol and of benzoic acid to toluene. A better result is obtained using rhenium oxide.[32] A quantitative yield is obtained at extremely high pressure in a long time.

The difficulty of working with finely dispersed catalyst leads often to the adoption of supported catalyst. It has been shown that supported rhenium does not show high selectivity towards the lactone, nor high conversion of levulinic acid, even in high temperature and high hydrogen pressure.[33]

Ruthenium catalyst

In more recent years the attention has been focused mostly on ruthenium catalysts, either in the metallic supported form on as a complex. It has been shown that it shows the highest activity in hydrogenating aliphatic ketones.[34] Osakada was the first to work with ruthenium phosphine complexes.[35] Total conversion and selectivity was claimed when working in the liquid phase (toluene solution) less than 12 bar of

hydrogen at high temperature (180 °C). The presence of the electron enriching phosphine is not necessary to the catalytic activity. A patent issued in 2002 reports high yield of lactone with a $[Cp^*Ru(CO)_2]_2^+OTf^-$ (Cp: $\eta^5C_5H_5$).[36] It should be noted that reaction pressure and time are high. Nevertheless it is possible to find in this paper many evidences of the activity of such a catalyst in the hydrogenation of ketones. Modification of the ligand leads to improvement on the stereoselectivity of the reaction. γ-valerolactone is an optically active molecule, though is often used as a racemic mixture. Starodubtseva et al. obtained optically pure enantiomers reducing ethyl, methyl and propyl esters of levulinic acid using ruthenium complex with an optically active ligand (BINAP).[37] The result was encouraging, both in terms of enantioselectivity (99 %) and yeld (95 %).

Working with homogeneous catalyst has many advances in terms of activity: every single metal atom is active in the reaction and there are few problems in terms of mass transfer of the reagent and of the product. Nevertheless it is usually difficult to separate the catalyst from the product stream. In the case of precious metals this is particularly important, and the catalyst recovery could be one of the most important parameters in the evaluation of the process economy. That is the reason why heterogeneous catalysts are often preferred. Since the discovery of the high activity of ruthenium complexes in the hydrogenation of levulinic acid two are the main ways researcher tried to overcome this problem. The first and preferred was to investigate if the high activity was maintained for the catalyst in the supported metal form, the second was to immobilize the ruthenium complexes on heterogeneous support in order to maintain the high activity, specificity and potentially also stereoselectivity on a catalyst characterized by single atom active sites.

Regarding the former, two patent issued between 1999 and 2003 reports the high activity of supported ruthenium, especially on carbon, along with a clear comparison of the catalytic activity of supported platinum, iridium, rhenium, rhodium and ruthenium, showing that the latter has the higher selectivity and conversion.[33,38]

This showed the possibility of working with a supported catalyst. Since then great attention has been paid to the understanding of the reaction conditions influence and to the solvent system, in order to ease a future industrial scale up.

DuPont patented a supercritical CO_2 system, that has the advantage of an easy separation of the reaction products, while operating at pressures that are reached with difficulty in the industry (250 bar).[39] The catalyst used was Ru/Al_2O_3 and the reaction was carried out in batch reactors for 2 hours achieving total conversion but not extraordinary selectivity (>75 %). The process worked at very high levulinic acid to carbon dioxide dilution (1:28) and the levulinic acid was pumped in the reactor as a 1,4-dioxane solution, making the separation of pure lactone potentially energy demanding. This patent was followed a few years later from a paper by Bourne, where levulinic acid was converted to γ-valerolactone in a similar setting but using milder conditions (100 bar of total pressure).[40] Ru/SiO_2 was used in this case and the new catalytic system achieved higher selectivity towards the lactone (99%). The separation of the lactone was in this case really easy and happened in the reactor. The behaviour of the γ-valerolactone-water-supercritical fluid mixture was similar to that of the one observed by Lazzaroni et al., i.e. a pure water phase separates from a THF-CO_2 phase in sub-supercritical conditions.[41] Nevertheless the hydrogenation happens with a large hydrogen excess of three times, while the patent described lower excess (20 %). Yan presented an extensive study of the influence of reactions conditions in the case of Ru/C catalyst.[42] The study presents the trends of the yield of the reaction in methanol as function of substrate concentration, hydrogen pressure, temperature, reaction time, catalyst loading, stirring speed and catalyst reuse. The systematic approach used was 'one variable at time' (OVAT). The study present precious information but the OVAT approach does not show the influence of a single variable on the other.[43] The same Ru/C catalyst has been used in a flow reactor setting, yielding high conversion and selectivity.[44] Raspolli Galletti et al. obtained 90 % yield working with a commercial Ru/C catalyst in the present of a solid-acid co-catalyst working at very low temperatures and pressures (70 °C, 5 bar).[45] Moreover, the hydrogenation is performed on a concentrate (50 %) water

solution. Using a similar flow setting but working in dioxane solution at higher temperature, Upare demonstrated that conversion and selectivity are almost total and constant for up to ten days.[46] Ruthenium catalyst activity was recently confirmed also when the metal is present in form of nanoparticles suspension.[47]

Bi-metallic ruthenium catalysts were studied in a few papers. Outstanding results, especially in terms of catalyst stability over time, were obtained working with ruthenium-tin alloy-nanoparticle supported on carbon.[48] The reaction was conducted in alkyl phenol solvent, because it has been found that this solvent extracts readily the levulinic acid from acid aqueous solutions, i.e. those where cellulose is converted to the acid.[49] This catalyst was stable over 10 days on stream and it showed lower activity compared to the monometallic catalyst but higher stability over time and higher selectivity. The monometallic catalyst, when used in this system, led to the hydrogenation of the solvent, while the RuSn catalyst is 100 % selective to GVL. During the first 5-10 hours on stream the activity of this catalyst was 75 % lower than that of the ruthenium catalyst. RuSn/C catalysts were stable up to 300 hour, while the corresponding monometallic was almost completely deactivated during that time. This result inspired a study on the economy of a process starting from cellulose and based on alkyl phenol separation and RuSn/C hydrogenating catalyst.[50,51] It has been shown that the process is economically sustainable if heat exchangers are well designed and that energy needs of the process, both in term of electricity and heat, could be fulfilled burning some of the biomasses. Up to date this is the only paper dealing with bimetallic catalysts where one of the two metals is ruthenium, and one of the few where bimetallic systems are treated.

In contrast to the main focus of the research on the hydrogenation of LA to GVL, Corma et al. showed the advantage of using a Ru/TiO_2 over Ru/C catalyst. The paper claims that the higher activity thus achieved arises from the interaction of the support with the carboxylic acid function that eases the reduction on the carbonyl group over the ruthenium nanoparticles. Furthermore the authors claim a lower

degree of metal leaching on a 0.6 wt.% Ru/TiO_2 catalyst compared with a 5 wt.% Ru/C, explained by the stronger metal-support interaction.[52]

The feasibility of a homogeneous ruthenium complex-catalysed process in aqueous phase was recently shown.[53,54] Very high selectivity and conversions were obtained when working with a sulfonated triphenylphospine ligand. The improved hydrophilicity of the ligand made possible the dissolution of the complex in water. The same complex was recreated in the heterogeneous form by mean of a polymer-bonded phosphine.[53] Although the catalyst becomes really easily recoverable when present in this form, it does not perform well in that experimental setting, showing a conversion slightly over 30 %.

Other metals

A gold catalyst supported on zirconia has been used for the hydrogenation of levulinic acid with molecular oxygen, and showed high yields.[55]

Very few researches deal with the hydrogenation of levulinic acid to γ-valerolactone using metals that are not noble. Copper has been used as a levulinic acid hydrogenating catalyst supported on zirconia. Working at high temperature and pressure (200 °C, 34 bar) it achieved total conversion. A paper published recently describes bi-metallic copper catalyst derived from hydrotalcites.[56] Among the catalyst tested copper-chromium and copper-aluminium hydrotalcite showed the highest activity, with yield up to 90 %.[57] This is due to the low electronegativity of chromium and aluminium that electronically enriches the copper catalytic centre; Cu-Fe hydrotalcite performs for this reason worse, catalysing further hydrogenation to methyl-tetrahydrofuran.[58]

Challenges

The current research has focused its attention on the tuning of the reaction conditions in order to achieve complete conversion of LA to GVL selectively. Very few publications have focused their attention on the reaction mechanism and on the

influence of the properties of the catalyst in the reaction yield. This kind of approach could be found mostly in publications dealing with homogeneous catalysts, where catalyst design allowed higher turnover numbers or higher selectivity, for example to the enantiomerically pure lactone.[37] In addition to that, no studies deal with the effect of the addition of another metal to ruthenium or with the presence of other functionalities on the catalyst.

A comparison between results obtained by different groups is difficult because in most of the cases different reaction conditions, analytical methods and experimental setup are used.

Furthermore, though achieving complete yield is surely important in the optimization of the overall process of transformation of lignocellulose into fuels, the presence of other steps must be taken into account.

The hydrolysis of cellulose or sugars to LA yields an acidic aqueous solution of various components, where LA ranges from 40 to 70 %.[59] A very small literature output is focused on the conversion of this kind of mixture, and the one-pot and/or one-step conversion of cellulose (or sugars) into GVL is even less represented. This kind of approach will surely limit the cost of separation of pure LA from the hydrolysis mixture, limiting expensive separations to successive steps. Most of the literature is focused on the conversion of a solution of pure LA in distilled water: the catalyst and the reaction conditions that proved to be the best in these conditions would probably perform differently on less pure substrates.

Precious noble metals have shown outstanding performances in mild conditions. Though a catalyst based on non-noble metal is usually cheaper, there are no studies that compare the cost of operating a process with noble and non-noble metal taking different operating conditions and catalyst life into account.

Aim of the project

The aim of this master project is to test different active phase compositions for the hydrogenation of levulinic acid to γ-valerolactone. Following the first steps of a catalytic process development, different catalysts based on different metals have

been prepared and tested to evaluate their performance with a consistent testing method.

In addition to that, Ru/C catalysts have been compared varying the support, the preparation method and the precursor used. Extensive characterization has been used to explain the different catalytic activity.

Table 1: LA hydrogenation to GVL literature data

reference	cat	solvent	Pressure (H_2)	Temperature	time	GVL yield
Schuette 1930[16]	PtO	ethyl ether	2.3-3 bar	Room temp	48 h	80 %
Kyrides 1945[18]	Ni raney	water	62 bar	180-200 °C	4,5	92%
Christian 1947[19]	Ni raney	no	35 bar	175-200 °C	3 h	94 %
Dunlop 1953[20]	Copper chromite	No, vapour	1 atm	200	Flow reactor	100 %
Broadbent 1959[31]	Re black	no	150 bar	106 C	18 h	71 %
Broadbent 1963[32]	Re(IV) oxide	No	200 bar	152 °C	12 h	100 %
Osakada 1982[35]	RuCl2(PPh3)3 RuH2(PPh3)4 RuCl(PPh3)3	Toluene	12 bar	180 °C	24 h	99 % 58 % 4 %
Elliott 1999[38]	5 % Ru/C	Dioxane	100 bar	120 °C	1 h	99 %
Bullock 2002[36]	$[Cp^*Ru(CO)_2]_2^+OTf^-$	DCB	57 Bar	90 °C	12 h	90 %
Manzer 2003[33]	5 % Ir/C 5 % Pd/C 5 % Rh/C 5 % Ru/C	Dioxane	55 bar	215 °C	2 h	95 % 70 % 96 % 97 %
Manzer 2004[39]	5% Ru/Al2O3	Water	100 bar CO_2, 150 bar H_2	150 C	2 h	99 %

Starodubtseva 2005[37]	Ru(COD)(MA)2—BINAP—HCl[1]	EtOH	60-70 bar	60 °C	5 h	95 %
Bourne 2008[40]	5% Ru/SiO2	Water	100 bar ($scCO_2$)	180-200 °C	Flow reactor	73-100 %
Yan 2009[42]	Ru/C	Methanol	12 bar	130 °C	3-4 h	>90 %, >90 %
Serrano-Ruiz 2010[44]	Ru/C	Water	35 bar	150 C	WHSV 4.8 h-1	96 %
Luque 2010[60]	Ru/Starbon	EtOH/water	10 bar	100 °C	2.1 h	95 %
Upare 2011[46]	Ru/C Pt/C Pd/C	Dioxane	1-25 bar	265 °C	50 h	98 % 90 % 30 %
Di Mondo 2011[61]	HOTf/316SS	Water	55 bar	70-100 °C	24 h	100 %
Primo 2011[52]	0.6 % Ru/TiO2	Water	35 bar	150 °C		93 %
Castelijns 2012[62]	Ru/C	No	20 bar	130 °C	1 h	79 %
Delhomme 2012[53]	Ru PPh3	Water	50 bar	140 °C	5 to 24 h	99/97%
Tukacs 2012[54]	Ru Bu-DPPDS	Water	10 bar	140 °C	4.5 h	99 %
Wettstein 2012[48]	RuSn/C	2-secbutyl-phenol	35 bar	180 °C	WHSV 1.2 h^{-1}	100 %
Raspolli Galletti 2012[45]	Ru/C solid acid cocatalyst	Water	5 bar	70 °C	3 h	98 %
Hengne 2012[63]	Cu/ZrO_2	Water	35 bar	200 °C	5 h	99 %
Li 2012[64]	Ir pincher complexes	Ethanol	50 bar	100 °C	15 h	96 %
Selva 2012[65]	Ru/C	Water-Isooctane-Ionic liquid	35 bar	100 °C	4 h	100 %
Du 2013[66]	Ir/CNTs	Water	20 bar	50 °C	1 h	99 %

[1] COD: cyclooctadiene, BINAP 2,2′ bis(diphenylphosphino)1,1′ binaphthyl.

Luo 2013[67]	Ru/TiO2, ZSM-5, Nb2O5	Dioxane	40 bar	200 °C	4 h	92 % (Ru/TiO2)
Ortiz-Cervantes 2013[47]	Ru NPs	Water	25 bar	130 °C	24 h	99 %
Pan 2013[68]	Ru/MgO	EtOH	40 bar	250 °C	6 h	92 %
Raspolli Galletti 2013[59]	Ru/C solid acid cocatalyst	Water from hydrolysis	5 bar	70 °C	5 h	83 %
Yan 2013[56]	Cu hydrotalcites	Water	70 bar	200 °C	10 h	90 %
Yan 2013[58]	Cu-Fe oxide	Water	70 bar	200 °C	10 h	95 %
Yan 2013[57]	Cu-Cr oxide	Water	70 bar	200 °C	10 h	90 %
Yan 2013[69]	Pd/SiO2	Water	90 bar	180 °C	6 h	97 %
Yu 2013[55]	Au/ZrO_2	Water	40 bar	120 °C	2.5 h	100 %

1.2. Experimental

Chemicals

Chemicals used for catalyst preparation and for reactions are listed below.

Carbons (Darco G60, Cabot Vulcan XC72, XC721 and XC72R, Norit GCN3070, Norit ROX 0.8, Norit PDKA) were obtained from the producers. Multi walled carbon nanotubes (O.D. x L 6-9 nm x 5 µm, >95 % C) were purchased from Sigma-Aldrich.

5 wt. % Rh/Al2O3, 5 wt. % Pd/Al_2O_3, 5 wt. % Pt/C, 5 wt. % Pt/C, $HAuCl_4$ and H_2PtCl_6 solutions were obtained from Johnson Matthey

$RuNO(NO_3)_3$ solution (Sigma Aldrich, 1.5 wt. % Ru), $RuCl_3$ (Sigma Aldrich, 45-55 wt. % Ru), $Ru(acac)_3$ (Sigma Aldrich, 97 %) were used as ruthenium precursors.

Levulinic acid (Sigma Aldrich, 98 %) was used as received.

Product used as standards for calibrations were of analytical purity and purchased from Sigma Aldrich.

Catalyst preparation

Catalysts were prepared by wet impregnation, deposition precipitation and sol immobilization methods.

For wet impregnation catalysts, a solution of the precursor(s) was added to the support to obtain a paste and water was added if necessary. The catalyst was dried overnight at 110 °C and calcined for 3 h at 400 °C (20 °C/min ramp rate) in nitrogen or in a 5 % H_2/Ar mixture.

Deposition precipitation catalysts were prepared starting from slurry formed adding the support (2 g) to a solution of the precursor in water (120 ml). The pH was regulated to 9 through the addition of NH_4OH and the suspension was aged for 1 h at room temperature. After filtering and drying at 100 °C overnight the catalysts were calcined at 400 °C for 3 h (ramp rate 20 °C/min) in nitrogen.

Sol immobilization catalysts were prepared starting from a solution of PVA (10 mg) and precursor in water (800 ml). $NaBH_4$ is added to generate the sol. After 30 min

the support is added and the solution acidified to pH 2 with sulphuric acid. The catalysts were then filtered and dried overnight at 110 °C.

Catalysts testing

Experiments were performed in a 50 ml Parr autoclave, equipped with a Teflon liner. In a typical experiment the desired amount of catalyst was added to 10 ml of a solution of 5 wt.% LA/H_2O. The autoclave was closed, purged with nitrogen and with hydrogen. It was then heated to the desired temperature, pressurized and stirred at 1000 rpm. After the desired reaction time the autoclave was placed in an ice bath. When temperature reached 10 °C the gases were vented (possibly analysed) and the autoclave opened. The liquid phase was filtered and analysed.

Analysis set up

A GC equipped with CP-Sil 5CB (50 m, 0.32 mm, 5 µm) column and FID detector was used. The method was set up using a mixture of LA, GVL and other possible hydrogenation, condensation, dehydration and hydrocracking product in water. Namely:

1. levulinic acid
2. gamma-valerolactone
3. methyl-tetrahydrofuran
4. anjelica lactone
5. valeric acid
6. 4-pentenoic acid
7. 3-pentenoic acid
8. 2-pentenoic acid
9. pentyl valerate
10. acetic acid
11. acetone
12. formic acid
13. propionic acid
14. ethanol
15. methanol
16. 1- and 2-propanol

All the product were separated using the following method:

Injector: 200 °C, split 20, injection volume 0.5 µl;

Pneumatics: constant flow, 3 ml/min;

Oven:

1. 80 °C for 5 min
2. ramp to 200 °C at 5 °C/min
3. 200 °C for 3 min

FID:

- Sensitivity: 11
- He make up: 25 ml/min
- H_2: 30 ml/min
- Air: 300 ml/min

The retention times of the compounds were measured through the injection of a solution of each compound in water.

Though the GC is equipped with an autosampler the internal standard method was chosen to reduce error derived from any lack in the reproducibility of the injection. The internal standard was selected with the following criteria:

- It should not be one of the reactant or one of the possible reaction products;
- It should not interact with any of the products/reagent, nor with the solvent;
- It should give a different signal, i.e. is should have a different retention time.

Acetonitrile was selected as the internal standard.

Calibrations were performed injecting solutions of the compounds in different concentrations, after the addition of the standard. Attention was paid in preparing solutions with concentrations in the same range as the experimental one. Many author state that the hydrogenation of LA to GVL is very selective and thus working with 5 wt.% LA in water calibration for LA and GVL were performed in the 0-10 % range, while calibrations for the other products were in the 0-1 % range.

Good linear correlation factors were obtained in relative response *vs.* concentration plots, with $r^2>0.999$ for most of the compounds. The calibration curve for LA is reported in as an example.

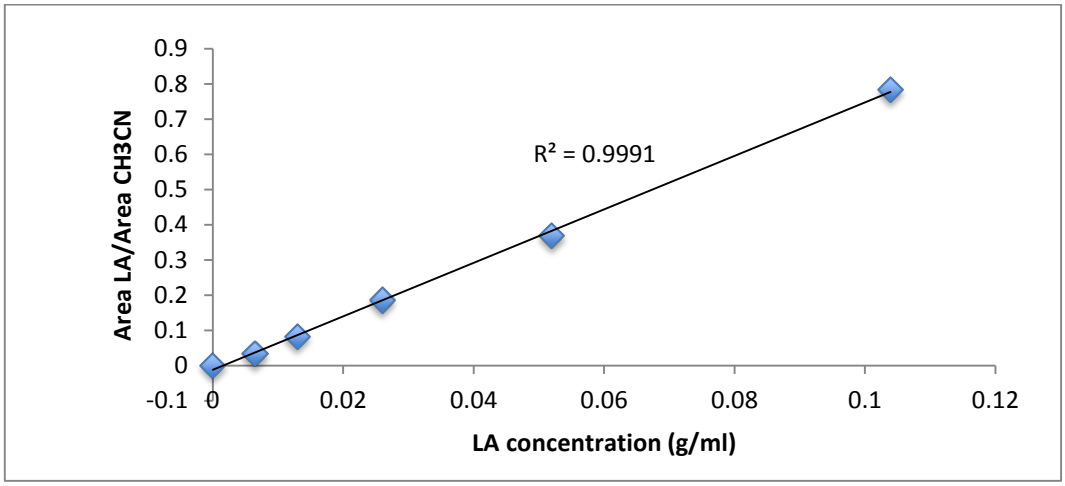

Figure 3: calibration curve for levulinic acid

Analysis of the products

When temperature reached 10 °C the gases were vented in a bag and analysed with a GC equipped with TCD and FID detectors and with a methaniser. Product in the gas phase always accounted for less then 0.1 % and therefore gas analysis was not always performed.

The liquid phase was filtered to remove the catalyst and analysed using a GC equipped with CP-sil column and FID detector using acetonitrile as the internal standard. Experimental error was determined to be below 5% by three repetitions of selected experiments.

Characterization

XRD were performed using a PANalytical X'Pert Pro fitted with an X'Celerator detector and a CuK α X-ray source operated at 40 kV and 40 mA, 2θ=10-80.

BET surface area analysis were performed after one hour degassing in helium at 120 °C using a Micrometric Gemini.

TPR were performed using a Quantachrome ChemBet equipped with a cold trap with 75 ml/min 5 % H_2/Ar, 10 °C/min ramp rate, TCD current set to 150 mA, attenuation 8.

CO chemisorption experiments were performed on a Quantachrome Chembet (sensitivity 150 mA, attenuation 1) after pretreatment at 250 °C in H_2 (50 ml/min, 15 min, 10 °C/min ramp rate) followed by purge with helium at the same temperature (50 ml/min, 15 min).

TPR data interpretation

The typical TPR for a Ru/C catalyst is reported in .

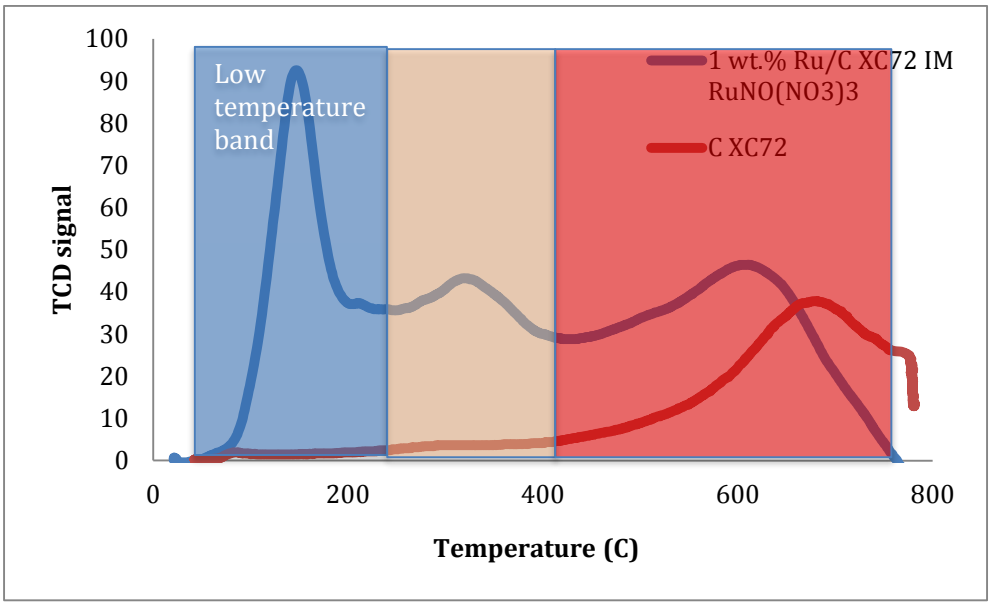

Figure 4: TPR of 1 wt.% Ru/C XC72 prepared starting from $RuNO(NO_3)_3$ precursor using an impregnation technique.

Three main peaks could be observed, whose assignment will be discussed in the next section. To integrate these peaks three gaussians are built according to the following equation. The software supplied by Quantachrome automatically performs these calculations.

$$I = I_0 e^{-\left(\frac{T-T_0}{a}\right)^2}$$

Where:

- I_0 is the maximum intensity of the band;
- T_0 is the temperature where the band is centred;
- a is a parameter related to the full width at half maximum (FWHM) of the peak according to the equation:

$$FWHM = a \cdot \sqrt{2ln2}$$

Once the three constants in the Gaussian distribution equation have been chosen in order to minimize the square of the residues $\sum(I - I_{exp})^2$ the integration is given by:

$$A = \sqrt{\pi} \cdot a \cdot I_0$$

CO chemisorption data analysis

Dispersion data are obtained through the calculations that are performed automatically by the TPRwin software.

The inputs that are required for these are:

1. Ambient temperature;
2. Ambient pressure;
3. Loop volume;
4. Catalyst mass;
5. Metal loading;
6. Adsorbent metal;
7. Adsorbate gas;
8. Titration profile.

1, 2 and 3 are used to calculate the number of moles for each pulse. Catalyst mass, metal loading and type of metal are used to calculate the number of moles of metal in the sample. Gas and metal types are required to determine the adsorption stoichiometry.

After recording the titration profile the user has to set the baseline for integration and select the pulse that will be used for calibration (those where no gas is adsorbed) and for calculation (those were total or partial adsorption occurred).

The software gives a result that includes the metal dispersion and metal specific area.

1.3. Results and discussion

Catalyst screening

Monometallic catalyst

The first part of the screening was devoted to a screening of the performances of different metals known for hydrogenation on carbon or alumina supports. The screening was performed in order to better compare the performance of the different catalysts using the same methodology. As underlined in the literature review, a comparison of the results reported for different metals in the hydrogenation of LA is difficult, because reaction conditions vary between different publications. The screening was performed in the following conditions:

Substrate	5 % LA in water
Temperature	120 °C
H_2 pressure	35 bar
Reaction time	4 h
Stirring rate	1000 rpm

Table 2:reaction conditions for the of the catalysts for LA hydrogenation

The results are reported in the following figure.

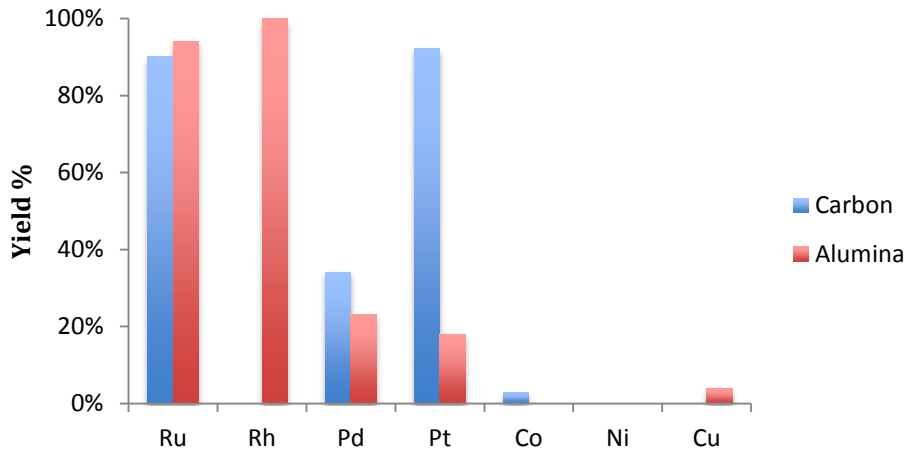

Figure 5: GVL yield of different 5 wt% metal/support catalysts. Reaction conditions: 10 g of 5 wt% LA/H_2O, 50 mg catalyst, 120 °C, 35 bar H_2, 4 h.

Ruthenium showed interesting results on both supports. Rhodium and platinum showed high yields but catalysts based on these two metals were not studied further owing to their high price. In the case of platinum it is interesting to note the different

activity on the two different supports, showing a negative influence of the Lewis-acidic behaviour of the alumina support, depleting electronic density from the metal phase. The metal-support interaction is stronger than that observed in the case of, for example, palladium and ruthenium catalysts where the difference between the two supports is smaller.

Ruthenium showed good results on both supports, while palladium yielded modest amount of GVL. It should be noted that in all cases the selectivity in the hydrogenation to GVL was almost complete (Figure 6), except in the case of the nickel catalyst, whose conversion was by the way less than 1 %.

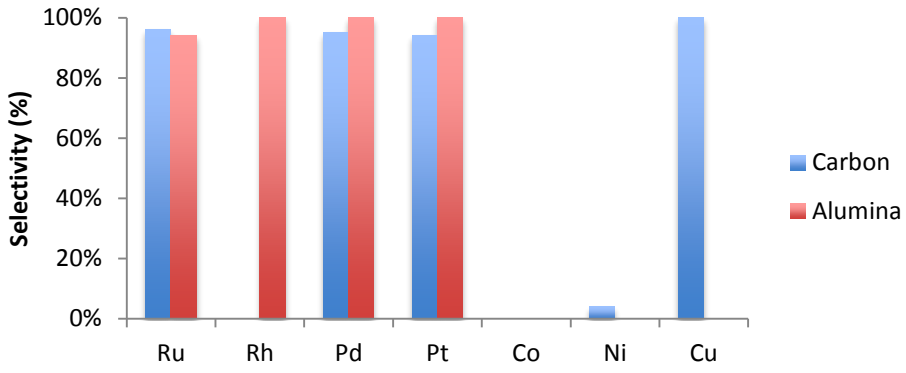

Figure 6: Selectivity of different 5 wt% metal/support catalysts. Reaction conditions: 10 g of 5 wt% LA/H_2O, 50 mg catalyst, 120 °C, 35 bar H_2, 4 h.

The performance of ruthenium and palladium catalysts have been evaluated also in the case of their alloy with gold

Bimetallic catalysts

Gold-palladium

The effect of the addition of gold to the palladium catalyst was investigated; gold palladium catalysts showed improved activity with respect to the monometallic catalysts in the selective oxidation of alcohols and in the direct synthesis of hydrogen peroxide.[70,71]

The results for gold, palladium and gold palladium catalysts are reported in table:

Table 3: Reaction conditions: 10 g of 5 % LA/H_2O, 50 mg catalyst, 120 °C, 35 bar H_2, 4 h.

Catalyst	**LA conversion**	**GVL selectivity**
5 % Au/C	**0%**	**-**
5 % Pd/C	**36%**	**95%**
2.5 % Au 2.5 % Pd/C	**87%**	**97%**

The presence of gold enhances the performance of the palladium catalyst in the hydrogenation of LA to GVL. Though these experiment showed interesting results a further study on the gold-palladium system was not performed because of the presence of catalysts with the same performances at a much lower price. Nevertheless some tests were performed to investigate if the addition of gold was somehow beneficial even to ruthenium.

Gold-ruthenium

Prepared gold ruthenium catalysts were tested in the standard conditions used for the catalyst screening. In this conditions a 2.5 wt.% Au 2.5 wt.% Ru/C catalyst prepared by impregnation led to complete conversion and selectivity. Yield versus reaction time curve was obtained for the 2.5 wt.% Au 2.5 wt.% Ru/C catalyst. Total conversion and selectivity were obtained for reaction times as short as 1 h.

Keeping the reaction time at 1 hour the pressure was decreased from 35 to 5 bar. As the yield stayed around 100 % the temperature was decreased. The conversion and selectivity vs. temperature are reported in Figure 7.

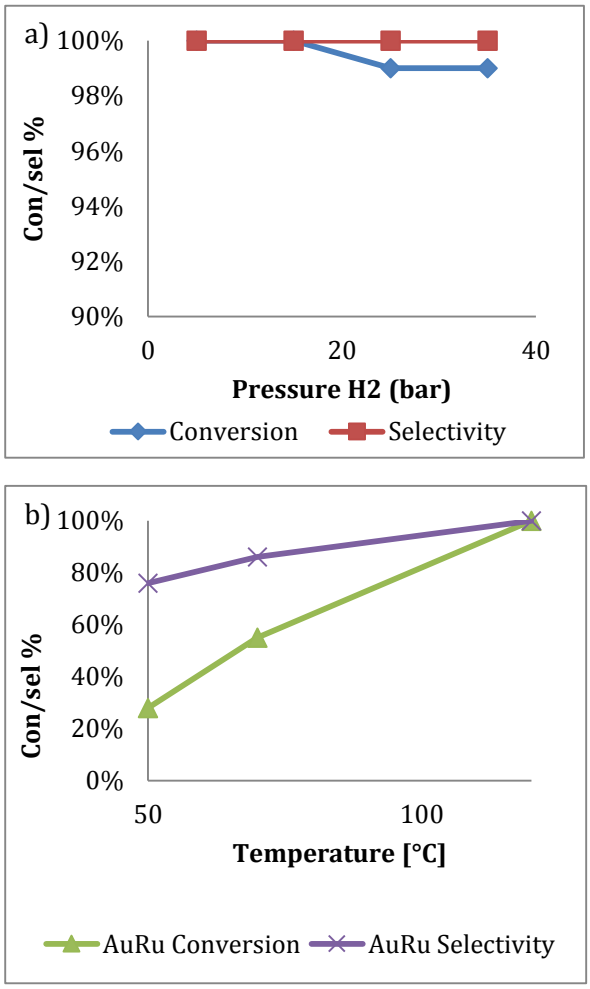

Figure 7. yield as a function of pressure (a) and temperature (b) for 2.5 wt.% Au 2.5 wt.% Ru/C. 10 g of 5 % LA/H_2O, 50 mg catalyst, 35 bar H_2, 1h

Comparison with the performance of the monometallic ruthenium catalyst was performed in order to evaluate the degree of any possible effect of gold. It must be noted from the binary phase diagram reported in Figure 8 that gold and ruthenium do not alloy at low temperature.[72] In particular, it can be noted from the phase diagram, that at ordinary temperature ruthenium is present as a pure metal at the equilibrium. This does not imply necessarily that gold exert no effect on the ruthenium. Though on the macroscopic scale the interfacial area between the two metals could be far too reduced to influence the properties of each phase, on the nanoscale the interfacial atoms could, depending on the average particle size, range up to more than 50 % of the total. The presence of an alloy is thus not necessary and the two different metals could interact effectively even when not alloyed. In addition to that the generation of the metal phase could create a metastable alloy. Furthermore the composition of the metal on the catalyst could be a metastable one.

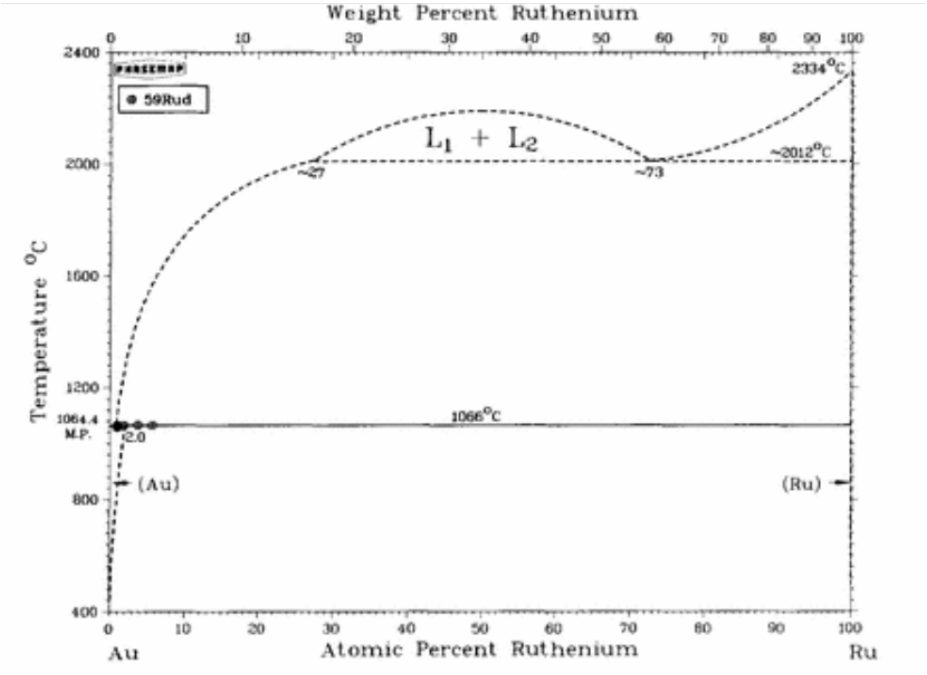

Figure 8: gold-ruthenium binary system.[72]

The comparison with the monometallic catalysts shows that gold improves the performances of ruthenium by a negligible amount. In the following table some

results are reported in terms of *turnover frequency* ($mol\ LA\ converted/(mol\ metal \cdot h)$) in order to compare the catalysts activity more easily.

Table 4: Result obtained with various Ru and AuRu catalysts

	Catalyst	Temperature (°C)	Conversion %	Selectivity %	TOF	TOF Ru[2]
1	5 wt.% Ru/C	70	97	87	>169	>169
2	2.5 wt.% Au 2.5 wt.% Ru/C G60	70	55	86	127	192
3	4 wt.% Ru 1 wt.% Au/C G60	70	97	96	187	>211
4	1 wt.% Ru/C G60	150	99	99	865	>865
5	1 wt.% Au 1 wt.% Ru/C G60	150	96	99	554	>838
6	0.5 wt.% Ru/C G60	150	42	99	733	865
7	0.5 wt% Au 0.5 wt.% Ru/C G60	150	49	99	559	846
8	0.8 wt% Ru 0.2 wt% Au/C G60	150	90	99	864	979

The catalytic results show that gold does not influence the performance of ruthenium. This could be noted comparing the results in terms of TOF referred to the number of ruthenium atoms for catalysts with the same ruthenium loading (entries 4-5 and 6-7).

Some of the gold-ruthenium catalysts were characterized using XRD and BET.

XRD show that gold and ruthenium are not alloyed in any of the prepared catalysts (Figure 9).

[2] *Turnover frequency based on the moles of Ru alone*

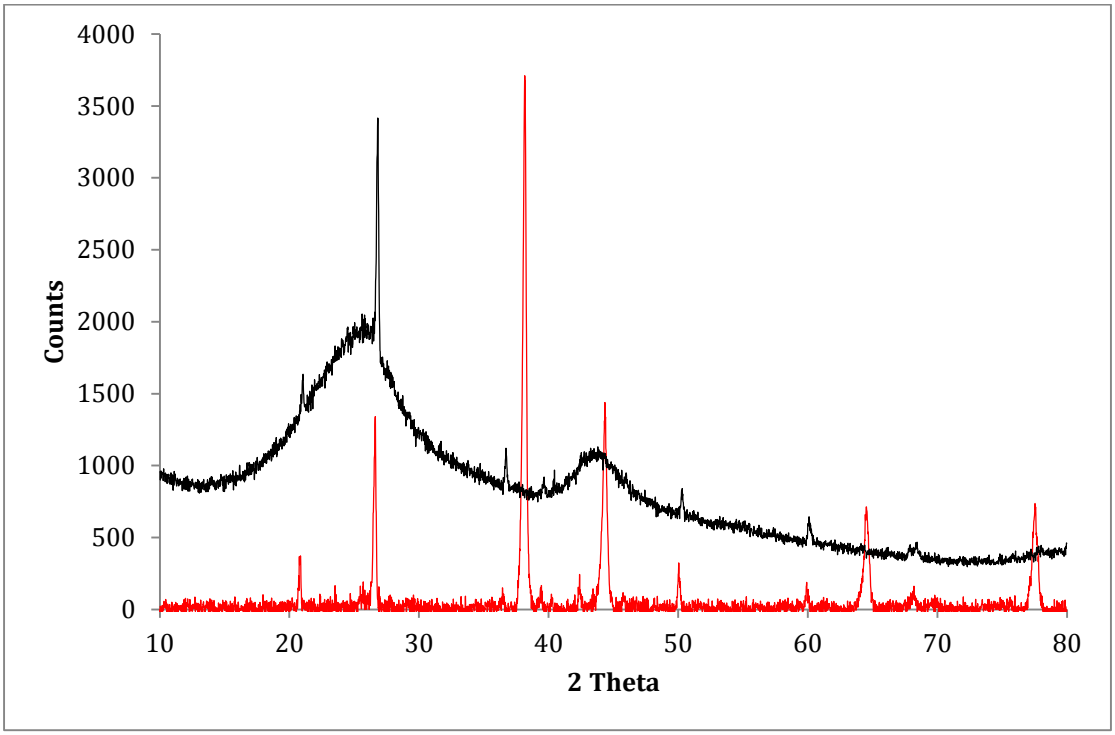

Figure 9: XRD of (black) 5 wt. % Ru/C G60 and (red) 2.5 wt.% Au 2.5 wt.% Ru/C G60.

The monometallic ruthenium catalyst does not show any peak corresponding to ruthenium, indicating high dispersion and very low particle size, while the AuRu bimetallic only shows peaks corresponding to gold metal nanoparticles. The high cost of gold (≈1600 USD/oz.[73]), along with the low performance increase, did not justify a further development of this catalyst.

Ruthenium is a cheaper metal (≈80 USD/oz.[73]) and it is remarkably active in the hydrogenation of aliphatic ketones, both as a homogenous and as a heterogeneous catalyst. When it is supported on carbon very high dispersions (>80 %) are observed.[74,75]

Other bimetallic catalysts

In order to complete the screening, bimetallic catalysts were prepared starting from the nitrates by wet impregnation. As underlined in the introduction not many information are reported about ruthenium bimetallic for the hydrogenation of levulinic acid. Tin-ruthenium showed very good selectivity in this reaction using alkyl

phenols as the solvent, avoiding the hydrogenation of the phenol ring and showing good stability.[48]

The results are reported in the following graph.

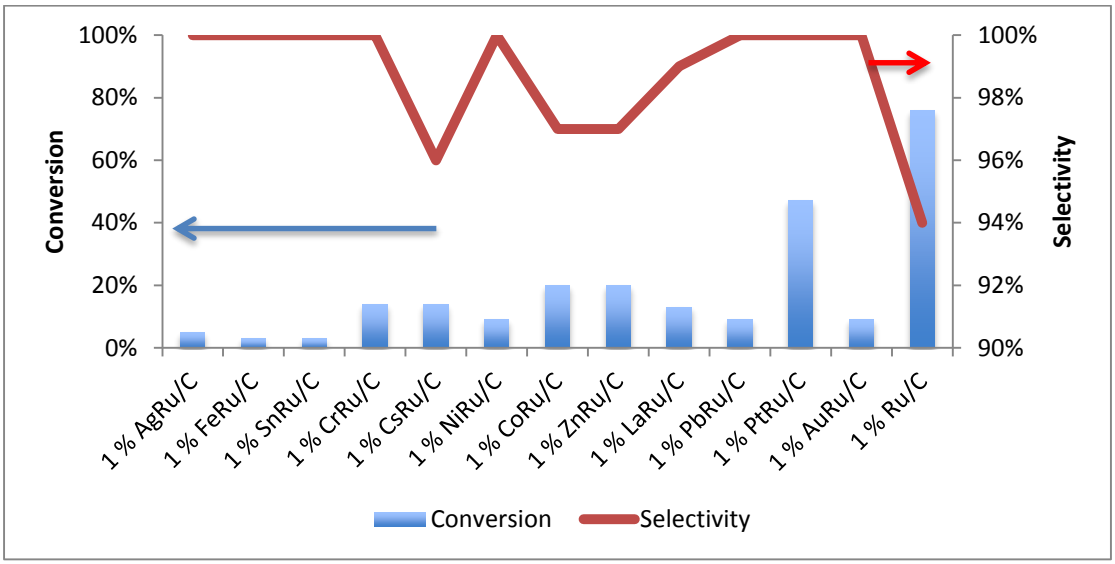

Figure 10: comparison of different 0.5 wt% Ru 0.5 wt.% Me/C XC72 bimetallics. Reaction conditions: 100 °C, 5 bar H_2, 10 g 5 wt.% LA/H_2O, 25 mg catalyst.

It is interesting to note that in most of the case the performance of the catalyst is heavily influenced by the addition of the second metal. In the following table the range of composition for the second metal (Me) in a MeRu alloy is reported, at standard temperature and pressure (data in weight percentage).

Table 5: weight composition range for Me in a MeRu alloy

	Ag[76]	Fe[77]	Sn[78]	Cr[79]	Ni[80]	Co	Zn[81]	Pt[82]	Au[72]
Alloy with Ru?	< 1 %	0-50 %	< 1%, Ru_2Sn_3, Ru_3Sn_7	0-30 %	0-5 %	100 %	100 %	100 %	<1 %

The composition used for the preparation of the RuSn catalyst the composition of the metal phase, at the equilibrium, is Ru_2Sn_3 (80 %) and pure Ru (20 %), but the conversion is rate is just 4 % compared to the 1 % Ru/C. The results obtained for the hydrogenation of LA to GVL in water with RuSn catalysts differ significantly from those reported by Dumesic et al. in alkylphenol solvent, but it should be noted that the solvents properties are very different.

Ru/C catalyst tuning

Characterization of the support

Carbon, both as carbon black and activated charcoal, is a very particular support that is characterized by the presence of many different surface functional group and many are the parameters that should be taken into account when characterizing it:

- Type and distribution of surface oxygen groups (hydroxyl, carbonyl, carboxyl…);
- Type and distribution of nitrogen group (aminic, amidic…);
- Micropore volume and total pore volume;
- Presence of other etheroatoms;
- Ionic impurities;
- Ashes.

Therefore the complete characterization of an activated carbon is particularly time consuming.

In order to investigate the most represented functional groups diffuse reflectance infrared spectroscopy (DRIFT) was performed on G60 and XC72 supports. The resulting spectra are reported in Figure 11.

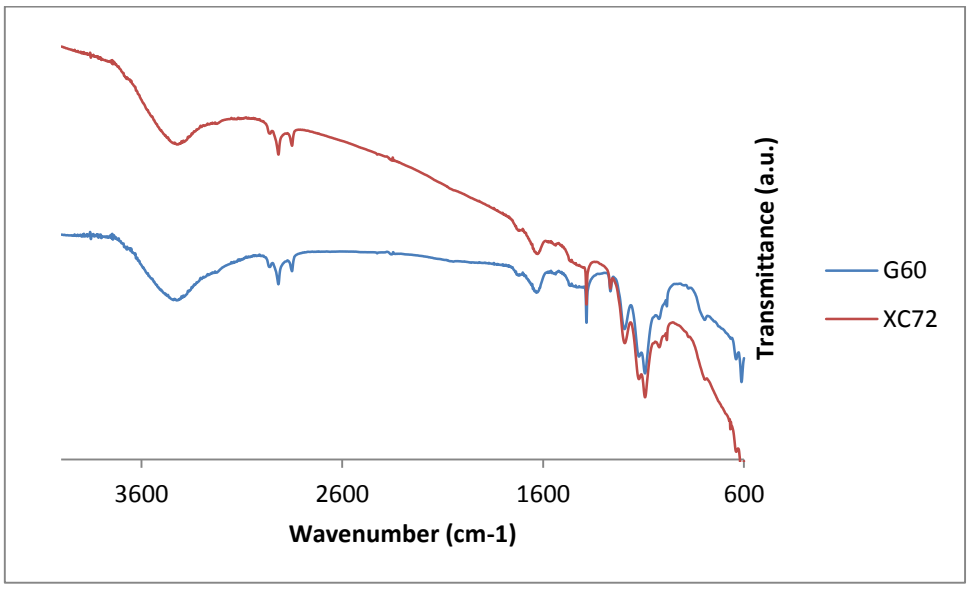

Figure 11: DRIFT of G60 activated carbon and XC72 carbon black

Presence of reducible group was investigated using TPR. In the following figure the same amount of two supports has been analysed. The amount of hydrogen consumed in the TPR could be also evaluated visually.

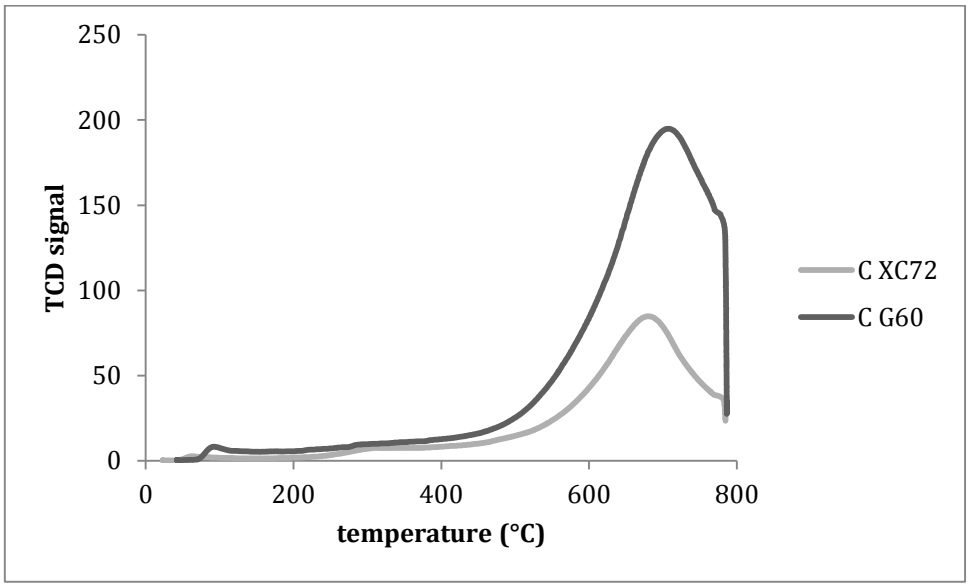

Figure 12: TPR of XC72 carbon black and G60 activated carbon.

The integration of the two curves shows that the hydrogen consumed for the reduction of G60 is 2.38 times that used for the reduction of the carbon black. To help gaining a better understanding of the distribution of reducible groups on the surface specific surface area measurements were performed using nitrogen adsorption with the BET method. The results obtained for Cabot Vulcan XC72 and Darco G60 are 210 and 670 m^2/g respectively (ratio=3.2). This difference is due to the different kind of materials, activated carbon having a more porous structure.

It is possible to combine data obtained from IR, BET and TPR. The infrared spectra cannot be used to get quantitative data, but suggest that the various groups are similarly distributed in the two supports. Quantitative data from TPR and BET indicate a similar surface density of reducible group, possibly slightly higher in the carbon black.

TEM and pore distribution measurements could help completing the characterization of these materials, along with EDX.

Catalytic data

Ruthenium catalysts have been widely investigated for the hydrogenation of levulinic acid to GVL. They showed higher activity compared to most of the other metals known for hydrogenation, as shown in the introduction. Furthermore in the cases that have been investigated the addition, by simple impregnation of the support, of a second metal does not improve conversion or selectivity. Amongst the other active metals investigated ruthenium is the cheapest one. As underlined in the introduction, most of the research has been performed using commercial catalysts, tuning the performance of these catalysts in different reaction systems, using different solvents, concentration of substrate, reaction conditions and cocatalysts.[42,45,73] None of the papers currently published focused the attention on the characteristics of the catalyst, as for example the type of support, the preparation method or the ruthenium precursor used for the preparation.

In the following paragraphs a tuning of the catalyst, followed by characterization of support and of the active phase, is exposed. The idea is to maximise the TOF of the catalyst and to correlate different values of activity to a different characterization.

A preliminary tuning of the reaction for monometallic ruthenium could be found in the section devoted to gold-ruthenium bimetallics (page 29). Results showed that a ruthenium catalyst, supported on Darco G60 carbon, yields complete conversion at 150 °C in 1 hour (Table 4).

To better compare the catalysts reaction conditions were chosen in order to have a GVL yield around 50 % with the standard 1 wt.% Ru/C G60 prepared by impregnation using $RuNO(NO_3)_3$ as a precursor (LA/Ru=1740, 100 °C, 5 bar H_2, 1 h, 1000 rpm)

1 wt.% Ru/C: influence of the support

Influence of the carbon support was first investigated. Many 1 wt.% Ru/C catalysts were prepared on different commercial supports. For the sake of comparison reaction conditions were tuned in order to achieve yields around 50 % for the benchmark 1 wt.% Ru/C supported on G60.

The Results are reported in Figure 13 in terms of TOF.

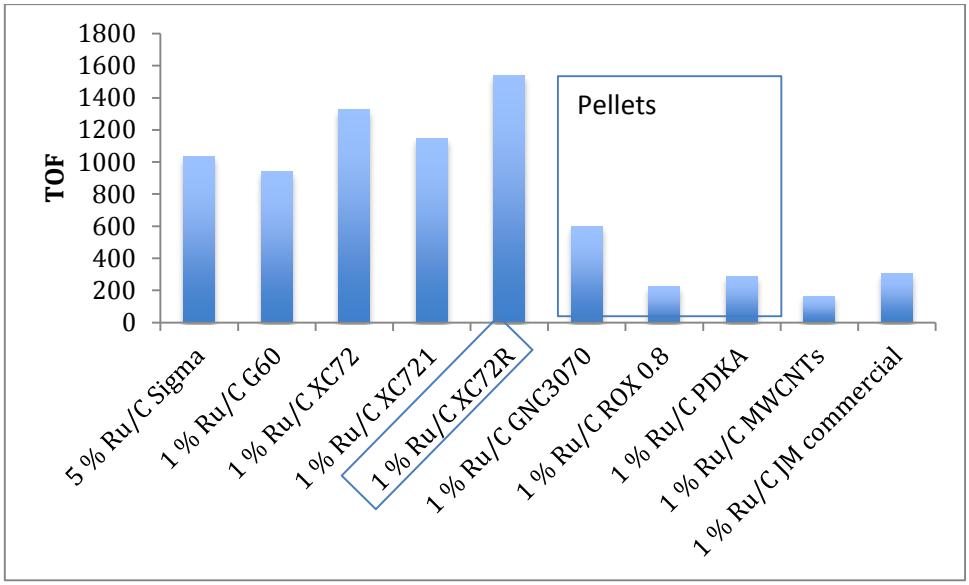

Figure 13: TOF results for some 1 wt. Ru/C on dfferent supports. Reaction conditions: 25 mg catalyst, 10 g 5 wt% LA/water, 100 °C, 1 h, 5 bar H_2.

Cabot Vulcan XC72-serie carbons showed remarkable activity, higher than the one showed by the commercial catalyst and from the activated carbons. Pellet shaped catalysts showed lower activity; this is probably due to more difficult mass transfer inside the porous solid. This lower activity must be balanced by other factor in order to justify development and use of pellet-supported catalyst. In particular, this kind of supports makes solid-liquid separation easier, and thus less expensive, and lower the pressure drop through a fixed bed. The performances of this catalyst are a good starting point for a continuous application, as a trickle bed reactor. On the contrary, carbon blacks are not very well suited for commercial application, because their very small particle size makes the recovery of the catalyst quite difficult.

Surprisingly, the catalyst prepared on XC72, i.e. the most active, show lower values of specific surface area. That implies that the surface area of the carbon is not the only key parameter determining activity, i.e. other characteristics must be taken into account, that influence both the form of the metal active phase and the reaction itself.

Supported ruthenium catalysts: influence of the preparation method.

The most representative supports that showed high activity value discussed in the previous were chosen in order to perform further studies. The influence of the preparation method on the catalytic activity has never been treated in the literature, but previous reports dealing with many different heterogeneously catalysed reactions underline its importance.

Three very well-known methods were chosen based on their high simplicity and reproducibility: wet impregnation, deposition precipitation and sol immobilization.

Catalysts were prepared with the same nominal metal load and tested in the same conditions described in the previous section. They all showed almost complete selectivity to GVL (>95 %), while differed significantly in terms of conversion. Catalytic data are reported in the following figures for G60 active carbon (Figure 14) and XC72R carbon black (Figure 15).

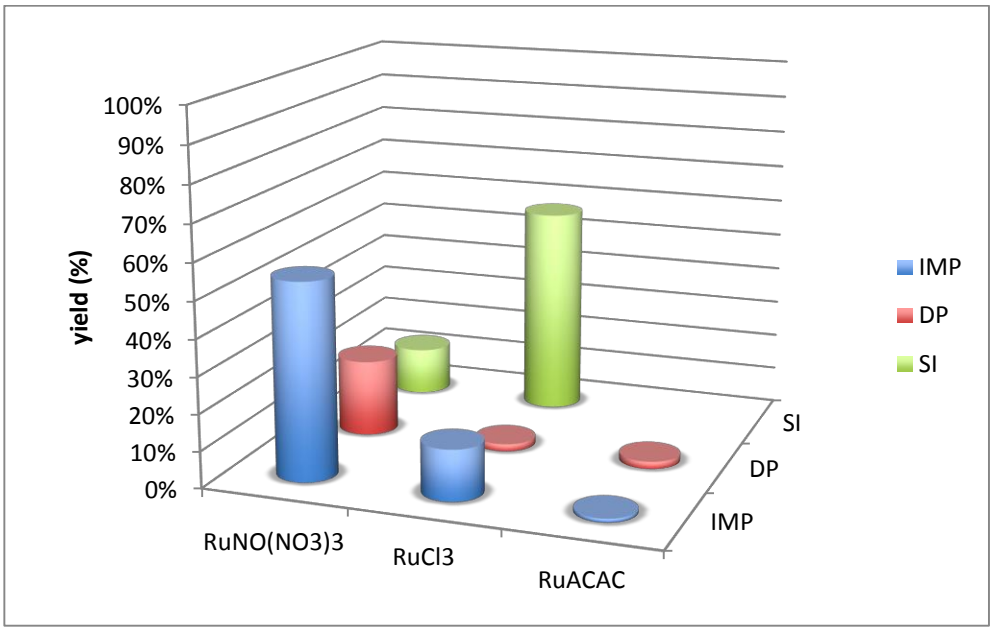

Figure 14: Yield results for different precursors and different preparation method on G60 carbon. Reaction conditions: 10 g 5 wt.% LA/water, 25 mg catalyst, 100 °C, 1 h, 5 bar H_2.

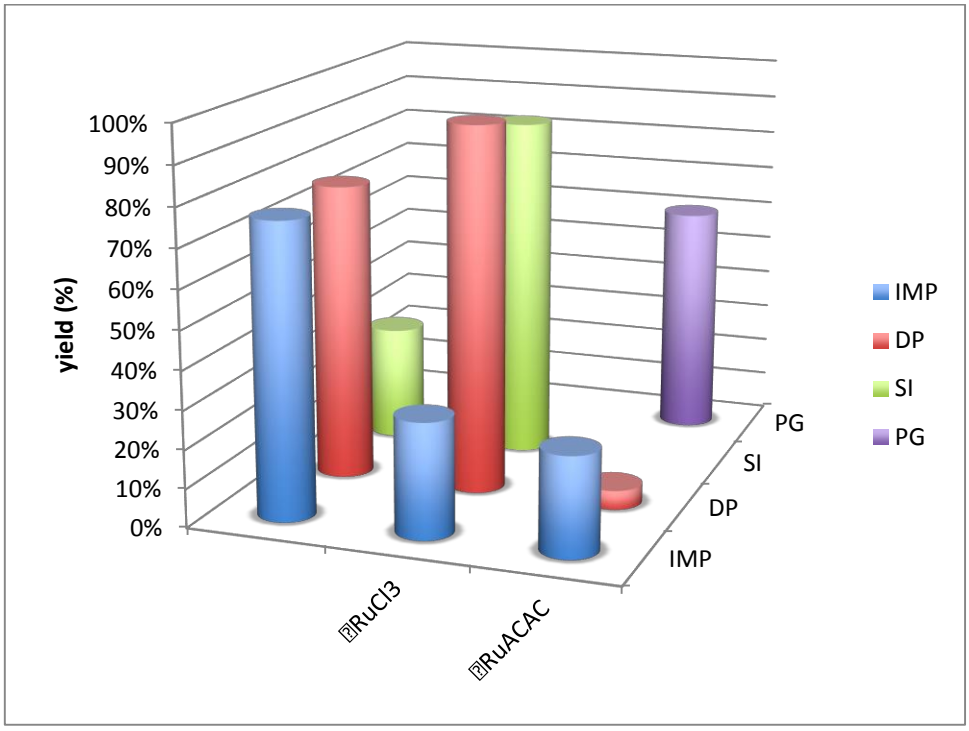

Figure 15: Yield results for different precursors and different preparation method on XC72R carbon. Reaction conditions: 10 g 5 wt.% LA/water, 25 mg catalyst, 100 °C, 1 h, 5 bar H_2.

The comparison between the two graphs shows a strong influence of the support on the catalytic performances of the differently prepared catalysts, XC72R carbon black being a better support. In addition to that other interesting information can be obtained.

High performances are obtained with impregnated catalysts starting from nitrosyl nitrate precursor that outperform those prepared from the chloride. Good results are achieved on both the supports using this simple preparation method and the difference could suggest that the counter ion of the metal influences dispersion and/or the active phase position on the catalyst, for example addressing the deposition on particular pore features (pore mouth etc.), or acting as a poison in the actual reaction.

Deposition precipitation catalysts show very low activity on G60 active carbon, while give high conversion when prepared on XC72R active carbon. It should be noted that the behaviour is different from that noted in impregnation catalysts, indicating a different role of the anion in the DP process.

Sol immobilization catalysts prepared from the chloride also showed very high yields. It is interesting to note that the preparation of these catalysts makes them different from the other reported in this study. The metal is obtained in the metal form and a layer of capping agent, in this case PVA, covers it. This capping agent is reported to limit the access of reactant to the particle's surface and different strategies were employed to remove it from the particle.[83-85] Hutchings et al. have reported a simple reflux in water to be very effective in removing PVA from Au nanoparticles deposited on titania.[83] The conditions used for this treatment are very similar to the reaction conditions used in this study for the hydrogenation of LA to GVL, the high reaction rate could arise from the effective removal of the polymer in situ. An insight into this process could be obtained looking at the time on line study reported in Figure 16.

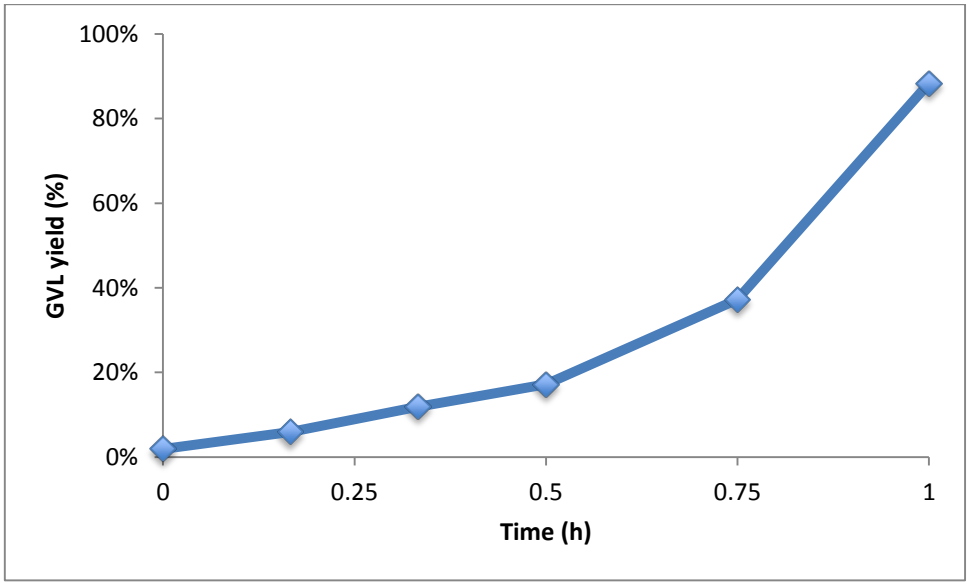

Figure 16: time on line for 1 wt.% Ru/C XC72R. Reaction conditions: 10 g 5 wt.% LA/water, 25 mg catalyst, 100 °C, 5 bar H_2.

The time online curve for 1 wt.% Ru/C made by sol immobilization from ruthenium chloride shows an induction period in the first 30 minutes. This could be due to the fact that the polymer exerts hindrance to the access of reactant to the metal surface. This capping agent layer is displaced by the action of the reaction mixture, resulting in an increase of the reaction rate.

The presence of the capping agent is usually very important in the case of small metal nanoparticles, because it impedes their agglomeration, minimising their

superficial free energy.[84] The removal of this component could result in a loss of stability. This is clearly shown by the stability test reported in Figure 17. The decreased activity observed, along with the stable selectivity, indicate that the number of active sites decreased upon reuse, while their nature remained unaltered.

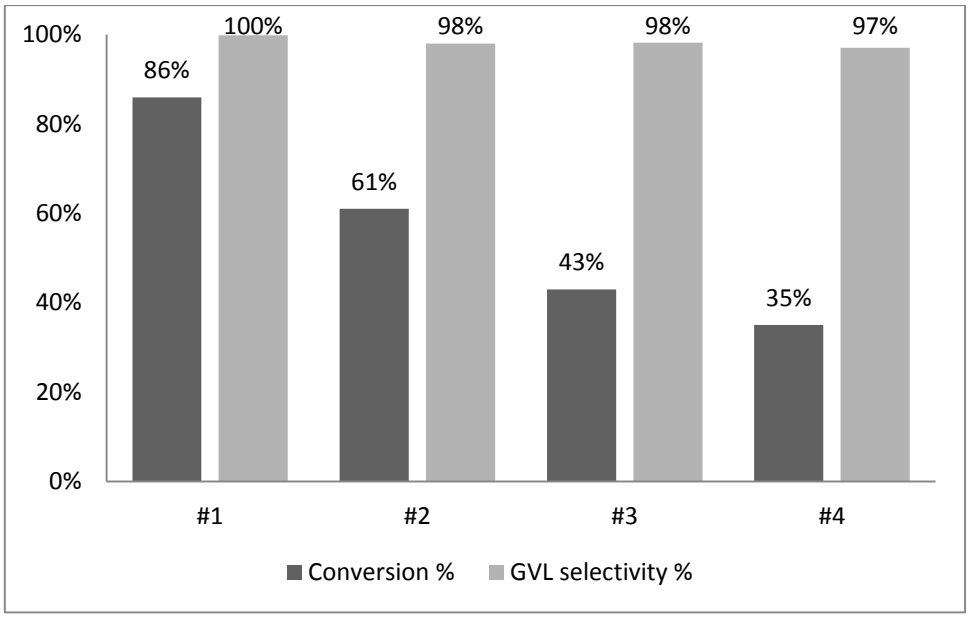

Figure 17: stability test for the 1 wt.% Ru/C SI Cl. Reaction conditions: 10 g 5 wt.% LA/water, 25 mg catalyst, 100 °C, 5 bar, 1 h, 5 bar H_2.

Catalysts prepared by impregnation starting from the nitrosyl nitrate have better stability though they show a lower initial activity (Figure 18).

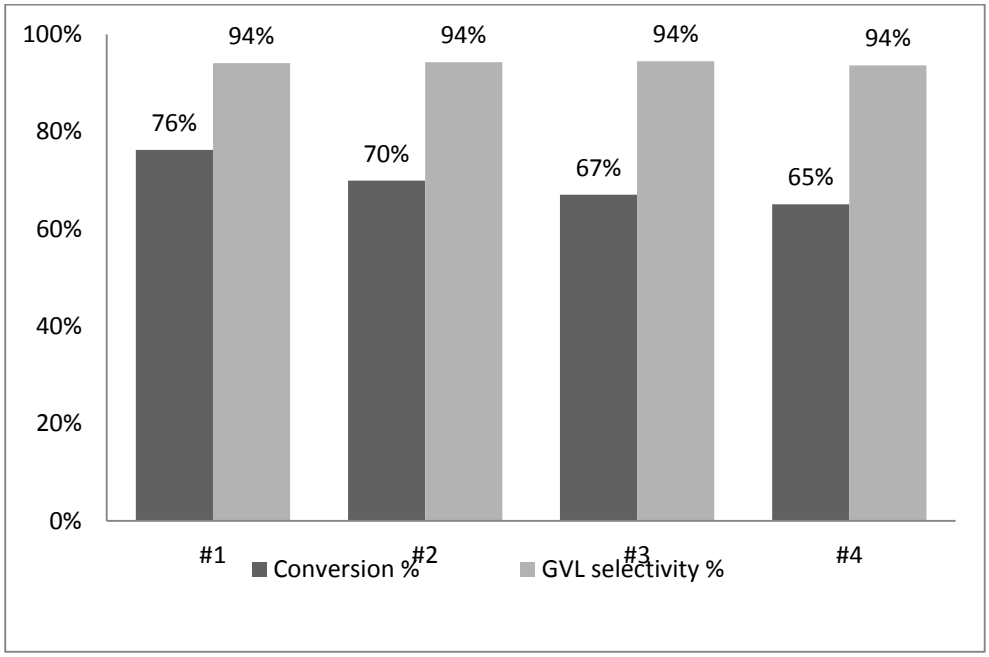

Figure 18: stability test for the 1 wt.% Ru/C SI NO_3. Reaction conditions: 10 g 5 wt.% LA/water, 25 mg catalyst, 100 °C, 5 bar, 1 h, 5 bar H_2.

The higher stability of these catalysts could be attributed to the calcination step that is performed in this case.

The calcination step for impregnated and deposition precipitation catalysts is performed in inert atmosphere at 400 °C. The most represented species on the catalysts in this condition is the oxide (RuO_2).[86] This could mean that the active catalysts are able to be formed by reduction at reaction conditions and that the activity depends on the degree of reduction to the metallic state. In order to rule out a dependence of the activity on the initial state of the catalyst surface, the impregnation catalyst obtained from the nitrosylnitrate precursor has been treated with $NaBH_4$ directly before the reaction. The result shows no difference with the untreated sample. The reaction conditions are therefore enough to reduce readily the catalyst surface and difference in activity should be ascribed to differences in other catalysts features.

Another interesting information that could be obtained from Figure 15 is the fact that an active catalyst could be obtained by mean of a simple physical grinding of the support and the acetylacetonate precursor. No reports were found in the literature dealing with such a catalyst and the properties and stability need to be better

investigated to understand if it represents a suitable option for aqueous phase hydrogenations of biomass derivatives.

1 wt.% Ru/C characterization

Surface area data were obtained for all the catalysts and the results are reported in Table 6 and Table 7.

Table 6: BET surface area data for G60 supported catalysts

	Impr	DP	SI
No metal	681	641	654
NO3	649	687	628
Cl	671	681	609
ACAC	668	667	

Table 7: BET surface area data for XC72R supported catalysts

	Impr	DP	SI
No metal	215	204	201
NO3	204	196	199
Cl	212	184	200
ACAC	190	190	

It could be noted that the surface area in not influenced by the catalyst preparation procedure significantly.

XRD analysis was performed in order to gain information on the active phases present on the catalyst and on the average crystallite size. The resulting diffractograms, reported in , do not show any reflection associable to ruthenium or its compounds.

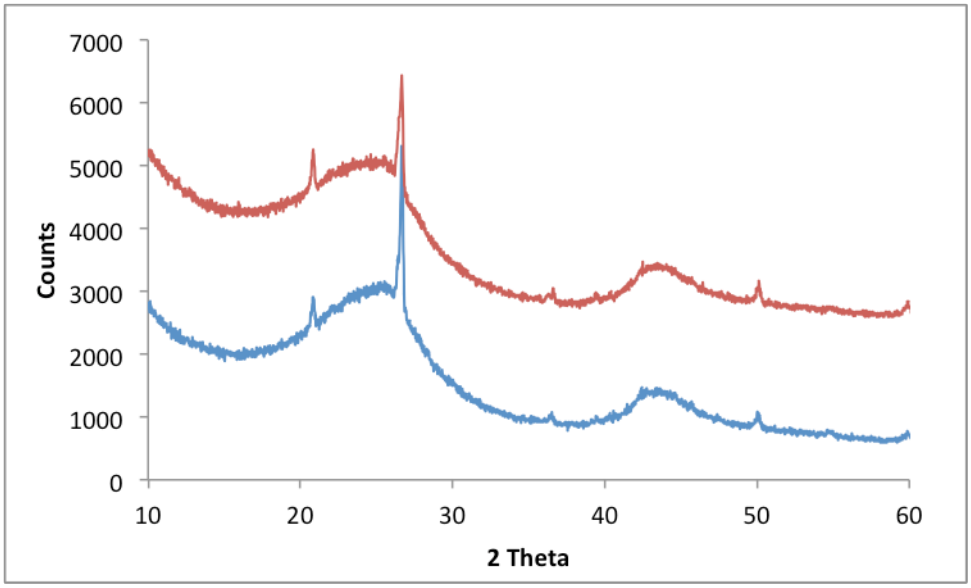

Figure 19: XRD of: G60 active carbon (blue), 1 wt.% Ru/C G60 IM NO3 (red)

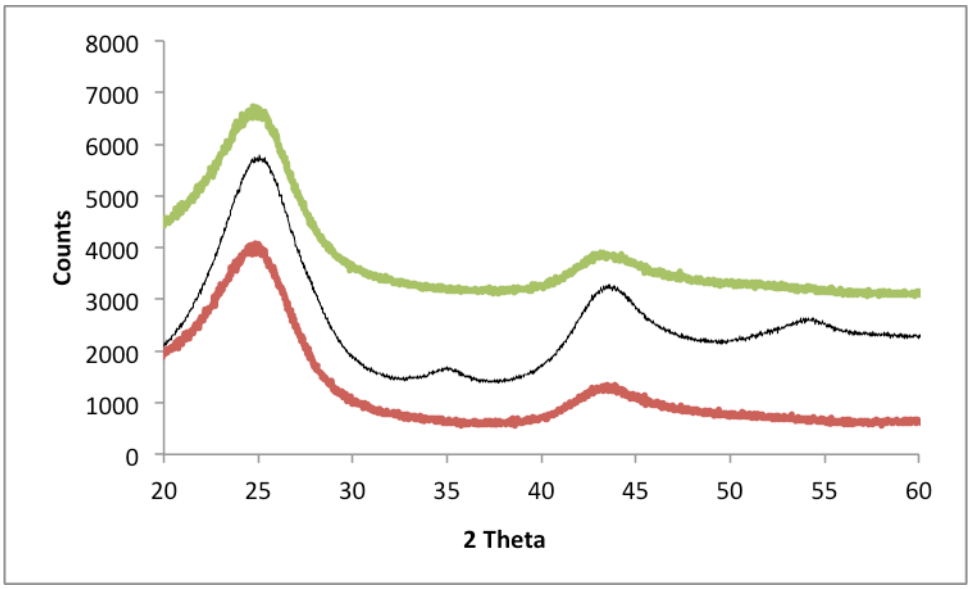

Figure 20: XRD of: XC72R carbon black (red), 1 wt.% Ru/C XC72R DP Cl (black), 1 wt.% Ru/C XC72R IMP NO3

The XRD analyses do not give much information. Amongst all the catalysts, the only one that show any reflection is the deposition precipitation prepared from the chloride. According to the Scherrer equation the average crystallite size in this case, based on the peak at 34 °, is 3.3 nm. It could be assumed that the other catalysts are made of smaller particles.

TPR and CO chemisorption techniques were used to gain further insight on the active phase oxidation state and on its surface. The first technique gives information about

the reducibility of the active phase composition and helps understanding the state of the surface in the reaction conditions.

Below a typical TPR curve for a ruthenium catalyst is shown along with the curve of the support.

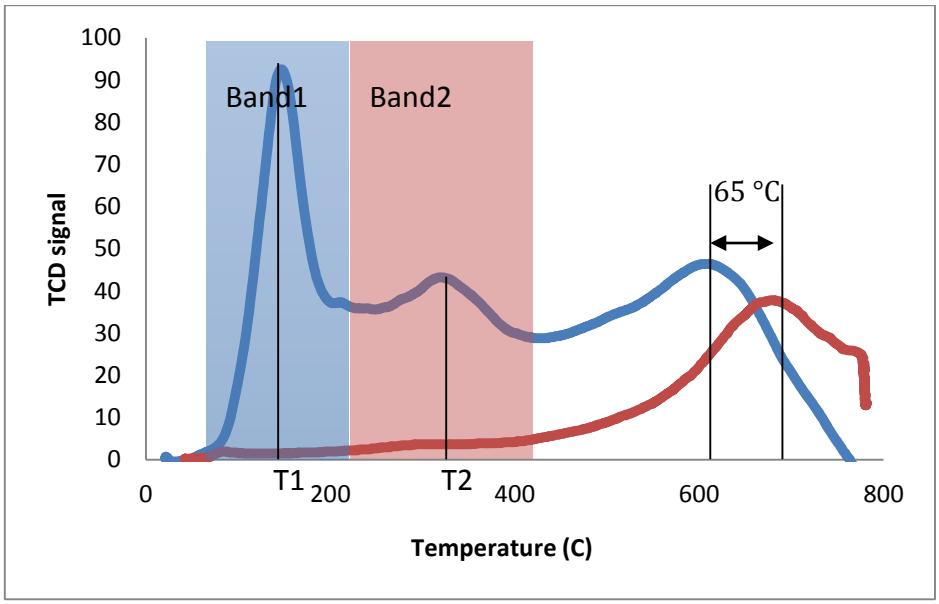

Figure 21: TPR profile for XC72R (red) and 1 wt.% Ru/C IM NO3.

Two main reduction peaks arise from the active phase, while the broad reduction peak of the support is generally shifted by 60-80 °C to lower temperature, probably due to a catalytic effect of the ruthenium metal on its hydrogenation.

The attribution of the other two peaks is still not clear and the literature typically attributes them as follows. The first low temperature peak is said to be either due to reduction of ruthenium oxide to the metal or to the reduction of Ru(IV) or Ru(III) to Ru(II), while the high temperature one is said to be due to the reduction of surface groups of the carbon support or to the reduction of Ru(II) to the metal.[74,86] Both these hypotheses are in contrast to the obtained data.

The first, that attributes the first peak to ruthenium and the second to reducible groups on the surface, is in contrast to the fact that the deconvolution and integration of the broad peak of the support gives the same value in terms of hydrogen consumption. This means that the second peak cannot be due to

hydrogenation of groups on the catalyst surface, unless this reduction follows another pathway when catalysed by the metal.

In the other case, if the second peak is to be attributed to the reduction of Ru(II), the results of its integration have to give a bigger or at least similar result, in order to respect the reaction stoichiometry.

It could be concluded that these peaks are due to different ruthenium species and further analyses are required to understand the starting status of the material. For example it is not possible to rule out the possibility of having species different from the oxide (nitrates, halides).

A relationship between the relative integration of the two bands and the activity could be obtained. The following Figure 22 represent the catalytic activity, expressed as GVL yield plotted against the percentage of hydrogen consumed in the first reduction peak.

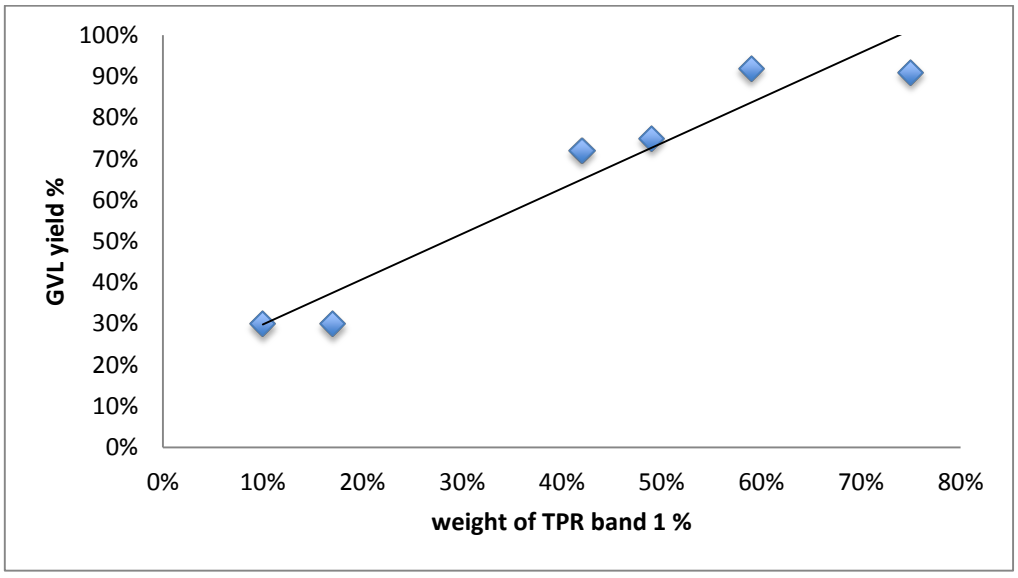

Figure 22: GVL yield as a function of the percentage of hydrogen consumed in the first reduction step.

It is interesting to note linearity between these two parameters. This could indicate that the most active catalysts are those that could be reduced the most in the reaction conditions.

1.4. Conclusion

The hydrogenation of levulinic acid to gamma valerolactone was performed in mild conditions (100 °C, 5 bar H_2) reaching almost full conversion and total selectivity to the desired product. Ru/C catalysts showed the best catalytic activity for this reaction.

The work demonstrated the possibility to increase the performances of these catalysts by mean of varying the preparation method and the support.

Regarding the latter, carbon black-supported materials shown superior activity compared to those prepared on active carbon, while having lower surface area. This implies a different metal-support interaction.

The preparation method was shown to have a dramatic influence on the performances. Catalysts prepared by sol-immobilization and deposition precipitation from $RuCl_3$ exhibited higher turnover frequencies compared to materials prepared by impregnation or commercial samples. The presence of an induction period in the catalytic activity of the sol immobilization catalyst suggests the possibility of the removal of the stabilizing polymer's layer due to the action of the reaction mixture. This removal lowers the stability of the particles, resulting in the important loss of activity over the first reaction cycles.

Dependence of catalytic activity has been studied in relation with many catalyst features. The BET surface area has a low influence on the yield of the hydrogenation, while TPR shows that there is good dependence between the amount of ruthenium reduced at low temperature and the activity in the hydrogenation reaction.

This work opens demonstrate the possibility of increasing the already high activity of ruthenium catalysts in the hydrogenation of levulinic acid to gamma-valerolactone and provides with a brief overview of some characteristics that could be typical of a good catalyst. At the same time many points still need to be investigated deeper.

Carbon has been shown to be a good support for ruthenium hydrogenation catalysts but a careful investigation should be performed to understand which are the characteristics that improve the activity of the active phase.

The preparation method has been shown to influence the performance of the catalyst drastically. An investigation based on microscopy and on surface analysis techniques must be performed in order to determine the structure-activity relationship and to design a better catalyst. Amongst this class of catalysts that perform better than the commercial ones, sol-immobilization Ru/C has to be taken into account though its stability has to be increased.

2. spectroscopic evaluation of metal nanoparticles accessibility using probe molecules

2.1. Introduction

Gold Catalysis

Gold has been considered inert in most chemical reaction for a long time. One of the first reports dealing with catalysis by gold is dated 1973, when Bond published a study on the hydrogenation of olefins.[87] Widespread studies on gold catalysis were initiated by two different discoveries, made simultaneously by Haruta and Hutchings in the 80s.[88,89] The first focused the attention on the low temperature oxidation of CO, while the second predicted gold to be an outstanding catalyst in the hydrochlorination of ethyne to vinyl chloride. Since then the research on gold-based catalysts proceeded with a high rate both as heterogeneous and homogeneous system (Figure 23).

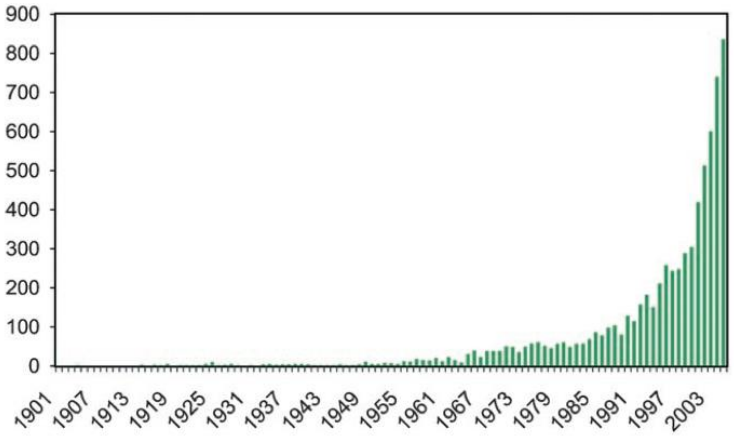

Figure 23: number of publication on "gold catalysis.[90]

With respect to heterogeneous applications gold has proved to be an effective catalyst for many reaction, especially selective oxidation. In addition to the oxidation of carbon monoxide, Haruta demonstrated the possibility of performing the direct selective oxidation of propylene to propylene oxide working with finely dispersed Au/TiO_2.[91] This reaction represents a very big challenge and is currently achieved in

the industry through process with low atom efficiency. Rossi reported the selective oxidation of polyols using Au/C, yielding α-hydroxy carboxylates in alkaline solutions with high selectivities, reduced metal leaching and stable selectivity values compared to palladium and platinum respectively.[92] Hutchings and co-workers demonstrated gold to be effective in the selective oxidation of hydrogen to hydrogen peroxide in non-explosive composition.[93]

Supported-gold catalysts preparation

Gold catalysts are usually prepared following the procedures used for supported metal catalysts. The most common are:

- Impregnation;
- Deposition-precipitation.

For the preparation of gold catalysts another important technique is sol immobilization.

In an impregnation preparation, the support is contacted with a solution of the metal precursor, usually in the form of a salt (nitrate, chloride…). The two most common impregnation techniques are:

- Dry impregnation or incipient wetness:

  The volume of the added solution is lower then the pore volume of the support. The results obtained with incipient wetness are usually well reproducible and the metal is mostly located in the pores of the prepared catalyst. The biggest issue with this methodology is due to the precursor solubility that could be not enough to achieve sufficient metal loading.

- Wet impregnation

  The volume of the solution of precursor that is added is higher than that of the pores. Additional care must be taken when preparing catalysts using wet impregnation to ensure reproducible results. In particular an interaction between the support and the precursor should occur.

The catalyst should then be dried, taking into account that the drying rate influences the metal position on the pore walls, and calcined in order to reduce the metal precursor.

Deposition precipitation gold catalysts are prepared through precipitation a carbonate or hydroxide gold specie. Usually, the pH of slurry containing the support and the precursor (usually $HAuCl_4$) is raised through the addition of a base (usually NH_3, Na_2CO_3 or urea acting as a delayed base through decomposition and formation of ammonia). The process should provide the precipitation of small particles inside the pores and care must be taken to avoid a rapid growth of the crystals that will impede their entrance into the pores resulting in deposition of bigger particles on the surface. The catalyst needs calcination to reduce the precipitate to metal.

Sol immobilization catalysts are prepared through immobilization of a metal sol on the support. A solution of $HAuCl_4$ and of a stabilizing agent (polymer, surfactant…) is prepared. A reducing agent is added to reduce the precursor to gold. After the sol generation step, the support is added to the sol and, upon a favourable electrostatic interaction between support and metal nanoparticles, the latter are immobilized on the former. This preparation does not require further treatments, because the metal is already present on the catalyst as such.

Sol immobilization provides a high dispersion of the metal with a narrow size distribution of nanoparticles (NPs) and the surface structure of the metal NPs is less influenced by the structure of the support than in the other preparation methods described.[83,94] These advantages, that involve the possibility of using lower metal loading, must be weighed with the fact that the metal in the obtained catalyst is still covered by the capping agent used in the sol generation step.[84]

Role of capping agent in metal nanoparticles preparation

Capping agents are used in the preparation of metal NPs in order to avoid over-growth and aggregation. These compounds could belong to different chemical classes, for example polymers (polyvinyl alcohol PVA, polyvinylpyrrolidone PVP, poly ammidoamine PAMAM…) or amphiphylic molecules (oleic acid, thiols…). They also

give the possibility of tuning the rate of crystallization in different directions because they adsorb differently on different crystal faces. While providing a better control of shape and size of the particles, these stabilizers have rarely a positive influence in catalytic applications.

The prepared metal nanoparticles have a core shell structure, where the inner core is constituted by metal and the shell is an organic layer composed by the capping agent that acts as a physical barrier to the diffusion of reactants to the catalytically active metal surface. Another problem could be the electrostatic incompatibility of reactant and capping agent.[95] Both results in reduced activity. It is often required to remove the stabilising agent before the reaction in order to achieve the best results.

Removal of capping agents from metal nanoparticles

Two different approaches can be used to have a clean metal surface on the catalyst, or at least to reduce the amount of physical hindrance and allow the reacting molecules to access the catalytic surface. The first is to use small molecules that are easily displaced in the reaction conditions as surfactants. Rossi et al. have successfully used this approach in the preparation of gold sols for the oxidation of glucose to sodium gluconate, using glucose as stabilizer. [96,97]

The second approach is to find a suitable technique to remove the capping agent from the prepared catalyst before performing the reaction. The organic molecule could be oxidised or removed using a suitable solvent.

Oxidation of the organic molecule has been performed with a high temperature treatment in oxidative conditions by Rioux et al. for the removal of PVP from Pt nanoparticles.[98] They demonstrated that a significant change in the shape of the nanocrystals happens at temperature (623 K) higher than those required for the degradation of the polymer (423-623 K). The behaviour of the oxidative degradation of PVP on Pt nanoparticles changes significantly from the degradation behaviour of bulk PVP, and it was demonstrated that degradation residues still stabilise metal nanoparticles. [99] Comparison of the results of the two researches suggests that while PVP is not completely removed, the treatment offers a better access to the surface.

Another method to eliminate PVP from Pt surface is its oxidation in UVO conditions, i.e. using ozone and UV irradiation, though it generates CO that is easily adsorbed on the catalyst and could poison it in certain applications.[100,101]

The use of a washing or refluxing treatment with a suitable solvent is performed in milder conditions, and could modify less the shape of the supported NPs. Hutchings and co-workers demonstrated the effective removal of PVA from titania supported gold catalysts using a simple reflux method with water as the solvent.[83] The removal of the polymer was demonstrated indirectly performing CO oxidation, benzyl alcohol oxidation and glycerol oxidation. The catalyst treated in water at 90 °C for 30-120 °C shown higher activity compared to catalysts calcined at 300-400 °C in hydrogen or air, while TEM data confirmed that the Au nanoparticles did not change their size significantly.

The solvent treatment was also applied to the removal of PVP from platinum sol. Blavo et al. treated the freshly prepared platinum sol with three consecutive cycles of ethanol-hexane washing at room temperature and proved the effective removal of PVP with temperature programmed oxidation and ethylene hydrogenation, after supporting the treated sol onto silica and titania.[85]

Removal of PVP from Au NPs has not been widely studied in the literature. Recently Ansar et al. used a solution of $NaBH_4$ to successfully remove PVP from gold sols and used surface enhanced Raman scattering and UV-vis spectroscopy to prove the fact that the polymer is removed and then slowly re-adsorbs on the metal sol.[102] Along with PVP the method proved to be effective with a wide array of organothiols.

There are no reports in the literature dealing with the removal of PVP from supported gold nanoparticles.

Tests to prove the effective removal of the capping agent

The greatest part of the literature regarding sol preparation of metal catalysts followed by a treatment to remove the capping molecules tests the effective accessibility of the metal surface performing a test reaction.[83,85] Comparison of the results for the treated and the untreated catalysts demonstrate the efficiency of the

treatment. Plots of the results of the test reaction varying the experimental conditions of the removal procedure help finding the best operating conditions.

Direct evidence for the removal of the capping agent is more difficult to obtain. As a matter of fact the mass of this species in the catalyst is similar to that of the metal and hence it accounts, in a typical preparation, to the 1 wt.%, and it is usually well dispersed on the catalyst. Classical spectroscopies (UV, IR, Raman) are not easily used to determine the variation in the content of the organic capping molecule. Nevertheless Hutchings et al. noticed a decrease in the intensity of Raman bands when performing the reflux treatment in water.[83]

UV-vis spectroscopy has been used to monitor the surface plasmon resonance band of gold upon adsorption of PVP and organothiols and desorption induced by $NaBH_4$.[102] UV-vis experiments were performed in transmission mode, because the work was performed on a gold sol.

Temperature programmed oxidation and thermogravimetric analysis were used successfully for Pt/Al_2O_3 and Pt/TiO_2.[85]

Up to date no reports deal with the use of a probe molecule to test the effective accessibility of the metal surface. For example the adsorption of CO on gold surface is very well known and well studied both with infrared spectroscopy and UV-vis spectroscopy, and many studies correlate the adsorption spectra of CO/gold with the activity of the catalyst for CO oxidation.

Diffuse reflectance infrared spectroscopy

Infrared spectroscopy is very widely used as an in situ technique. It can be performed in transmission mode, in the case of solutions, or in reflectance mode for solids. Among the reflectance techniques two are the most widespread, attenuated total reflectance (ATR-IR) and diffuse reflectance (DRIFT).

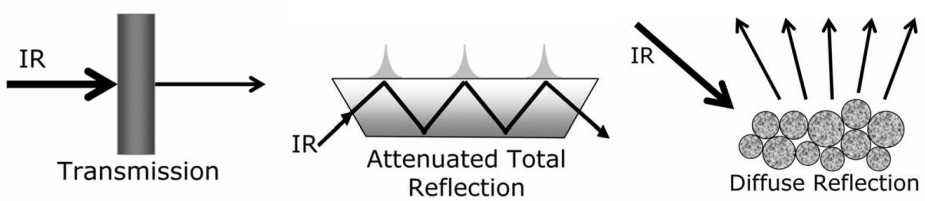

Figure 24: some of the possible IR analysis configurations.

While DRIFT is a very good technique for the analysis of oxidic powder, not much information could be obtained from metal nanoparticles.

A common technique to obtain indirect information of a material is the vibrational analysis of an adsorbate. In the case of gold it is interesting to observe carbon monoxide and how its stretching frequency is modified when environmental conditions and feature of the substrate are modified.

First observations are due to Yates in the late 60s.[103] A band for adsorbed CO was observed working with Au/SiO_2 and it was noted that the frequency of the stretching shifted to lower wavenumbers at higher CO partial pressure. Dumas et al. performed pioneering vibrational studies of adsorbed carbon monoxide in the 80s, where the shift that was observed at higher coverage was splitted in two components: a chemical one, due to the changes induced in the support by adsorbed molecule, and a coupling component due to the interaction between neighbouring adsorbed CO molecules.[104] The total observed shift was of -13 cm^{-1} (from 2125 cm^{-1} at low coverage to 2112 cm^{-1} at high), with the chemical one accounting for -30 cm^{-1} and the coupling for +17 cm^{-1}. These works were conducted on Au, Cu and Ag films. France investigated this effect and its two components further, obtaining the total, chemical and coupling shift in a wider CO partial pressure range.[105] Boccuzzi and Haruta have studied the adsorption of CO on gold catalysts prepared by deposition precipitation and showed how the vibrational frequency of the adsorbed CO band changes depending on the environment and on the nature of the sites.[106-108] Their results are in agreement with the previous literature: the drift of the band is due to different coverage at different CO partial pressure in the 2105-2118 cm^{-1} range, bands located at higher wavenumbers are due to partially positive $Au^{\delta+}$ sites, and are usually created upon calcination

Results discussed above are all obtained using transmission FT-IR. Grunwaldt and Bollinger have analysed Au/TiO_2 catalysts using DRIFT. Comparison with previous researches show that the data obtained are in good agreement with a transmission setup.[109,110] Furthermore the DRIFT setup could allow to heat or calcine the sample

'in situ'. Treatment in air at 400 °C generates positively polarised sites that upon adsorption of CO show a band in the 2128-2135 cm^{-1} range.

Diffuse reflectance UV-vis spectroscopy

Gold nanoparticles are particularly suitable to be studied through UV-vis spectroscopy. They show a typical band in the visible region that is due to the presence of the surface plasmon resonance (SPR). The adsorption is due to the resonance established when the frequency of the incident light matches the vibrational frequency of the electrons located on the surface of the particle.[111] In the case of nanoparticle the SPR is said localised surface resonance.

SPR frequency is very sensitive to changes in the environment and materials showing SPR are very well suited for applications in the field of sensing.[112] Many works deal with the development of sensors for the analysis of gas or with application in the biological field.[113-115] The typical setup is a thin layer of metal exhibiting the plasmon resonance covered with a layer of a selectively adsorbent material. In the biological field this technique is used for the recognition of specific macromolecules as proteins, RNA or DNA: the metal is hence functionalised with single stranded nucleic acids or with particular receptors. The adsorption event is measured by a change in the typical frequency of the plasmon resonance. Schematics for sensing of gases and macromolecules are reported in Figure 25.

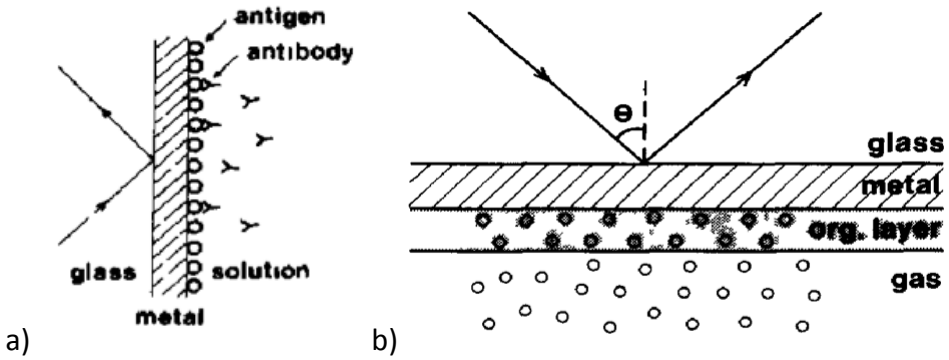

Figure 25: Setup for a) macromolecules sensing and b) gas sensing.

Characterization of gold-based heterogeneous catalysts through UV-vis spectroscopy is a very well known technique: many information could be drawn from the frequency of the band regarding the average size and shape of the particles.[112,116]

More rarely some groups focused their attention on the use of supported gold nanoparticles as gas sensors. Haruta has achieved this goal using Au/CuO and Au/Co_2O_3 using CO and H_2 as the probe molecules.[117-119] A linear relationship between CO concentration and variation in absorbance was established and small red shift of the band was observed on CuO. Sirinakis demonstrated the possibility of sensing CO at high temperature (above 400 °C) using gold on yttrium stabilised zirconia monitoring the shift in frequency of the SPR.[120] No sensing signal was observed at temperature lower than 400 °C and when working in anaerobic conditions, while a blue shift was observed in the presence of oxygen at high temperatures.

Aim of the project

Previous researches that were conducted in the group showed the possibility of removing PVA from supported gold nanoparticles by mean of a mild treatment in water at 90 °C.[83] The treatment was more effective than calcination and did not change the shape and size of the gold particles significantly.

The aim of the project is the determination and tuning of performances of the same treatment in the removal of PVP stabilized Au NPs immobilized on titania. The treatment is to be performed in different solvents and its effect will be compared with the effect of calcination. Verification of the removal of the polymer and of the gained accessibility of the surface will be verified in the room temperature oxidation on carbon monoxide. A deposition-precipitation catalyst will be used as a standard, to evidence the effect of treatment on an already active catalyst.

In addition to that diffuse reflectance UV-vis spectroscopy and IR spectroscopy will be used to determine the removal of the capping agent and other effects of the treatments performed both directly, i.e. recording spectra of the catalyst, and indirectly using CO and monitoring the effect of its possible adsorption on it own

vibrational characteristics and on the electronic features of the metal, through IR and UV respectively.

2.2. Experimental

Chemicals

Chemicals used for catalyst preparation and for reactions are listed below.

TiO_2 Degussa P25, was obtained from the producer, $HAuCl_4$ was obtained from Johnson Matthey.

PVA (MW 10000, 80 % hydrolysed), PVP (MW 10000) and $NaBH_4$ were purchased from Sigma Aldrich and were used as received.

Ammonium hydroxide (30 wt.%) was purchased from Fisher Scientific.

CO was purchased from BOC and was of analytical purity.

Catalyst preparation

Catalysts were prepared by deposition precipitation and sol immobilization methods.

Deposition precipitation catalysts were prepared starting from slurry formed adding the support (2 g) to a solution of the precursor (0.83 mM $HAuCl_4$) in water (120 ml). The pH was regulated to 9 through the addition of NH_4OH and the suspension was aged for 1 h at room temperature. After filtering and drying at 110 °C overnight the catalysts were calcined at 300 °C for 4 h (ramp rate 20 °C/min) in nitrogen.

NOTE: care must be taken in the precipitation of gold(III) with ammonia, because the highly explosive fulminating gold could be formed in certain conditions. Low metal loading and high dispersion of the precipitated precursor are factors lowering the risk. The possible advantage of the absence of alkali metal ions on the prepared catalyst must be weighed carefully with the intrinsic risk associated with the procedure and care must be taken in avoiding mechanical stress (shocks and grinding) on the dried catalyst before calcination. After calcination the catalyst will not present any risk, because the upper decomposition temperature of fulminating gold is around 220 °C.[121]

Sol immobilization catalysts were prepared starting from a solution of PVA (10 mg) and precursor in water (800 ml). $NaBH_4$ is added to generate the sol. After 45 min of

sol generation the support is added and the solution acidified to pH 2 with sulphuric acid. The catalysts were then filtered and dried overnight at 110 °C.

Catalyst treatment

Prepared catalyst were treated as follows:

90 °C solvent treatment

250 mg of the prepared catalysts were placed in a 250 ml round bottomed flask equipped with magnetic stirring and condenser and 125 ml of solvent were added. The mixture was heated to 90 °C in an oil bath and the treatment performed for 30, 60, 120, 240 min. In case of lower boiling point solvents or mixtures the treatment was performed at reflux conditions.

Calcination

The catalyst was calcined in static air for 4 h at different temperatures (20 °C/min ramp rate).

Ethanol-hexane treatment

The catalyst (250 mg) was placed in a flask and 30 ml of ethanol added. The slurry was stirred for 5 min and then 90 ml of hexane were added, stirring the mixture for 5 min. The stirring was then stopped and after settling the clear solvent was removed and the slurry at the bottom centrifuged. The treatment was repeated three times, followed by three cycles of washing with hexane and centrifugation of the catalysts. The powder was then dried overnight at 110 °C.

UV treatment

The catalyst was placed in a beaker with 120 ml of water. A 100 W UV lamp (254 nm) was then placed into the suspension and the mixture was stirred for 2 h. The catalyst was then filtered and dried overnight (110 °C).

Catalyst testing

Catalysts were tested for CO oxidation using a fixed bed glass reactor with 3 mm internal diameter placed in a thermostatic bath (25 °C). 5000 ppm CO/air was used as a gas and an electronic mass flow controller controlled the flow. CO oxidation product were analysed using a GC equipped with an automated injection valve and a TCD detector.

TOF (Turnover Frequency) is expressed as:

$$TOF = \frac{mol_{CO\ converted}}{mol_{Au} \cdot h}$$

In situ techniques

DRIFT-spectroscopy

All Diffuse Reflectance infrared Fourier Transform (DRIFT) spectra were recorded on a Bruker Tensor 27 spectrometer fitted with a HgCdTe (MCT) detector and a Harrick Praying Mantis HVC-DRP-4 cell equipped with KBr windows with the following settings: 64 scans, resolution 2 cm^{-1}, aperture 4 mm in the 600 to 4000 cm^{-1} range. Spectra were compensated for gas phase water.

Typically, the catalyst was placed in the cell in a nitrogen flow (50 ml/min) and the background recorded. The flow composition was changed to 1 % CO/N_2 or 1 % CO/air and a spectrum recorded after 10 min stabilization time.

The result spectra were obtained through subtraction of a spectrum obtained flowing 1 % CO/N_2 or 1 % CO/air on KBr.

Diffuse reflectance UV-vis spectroscopy

Reflectance UV-vis spectra were recorded on a Varian Cary 4000 spectrophotometer equipped with a Harrick Praying Mantis HVC-DRP-4 cell. The catalyst was placed in the cell and spectra were recorded in N_2, air, 1 % CO/N_2 or 1 % CO/air (50 ml/min).

2.3. Results and discussion

Water treatment of 1 wt.% Au/TiO2

1 wt.% Au/TiO_2 made by sol immobilization and stabilised by PVA (SI-PVA) or PVP (SI-PVP) and a 1 wt.% Au/TiO_2 prepared by deposition precipitation (DP) were treated with 90 °C water for different times. The results are reported in Figure 26.

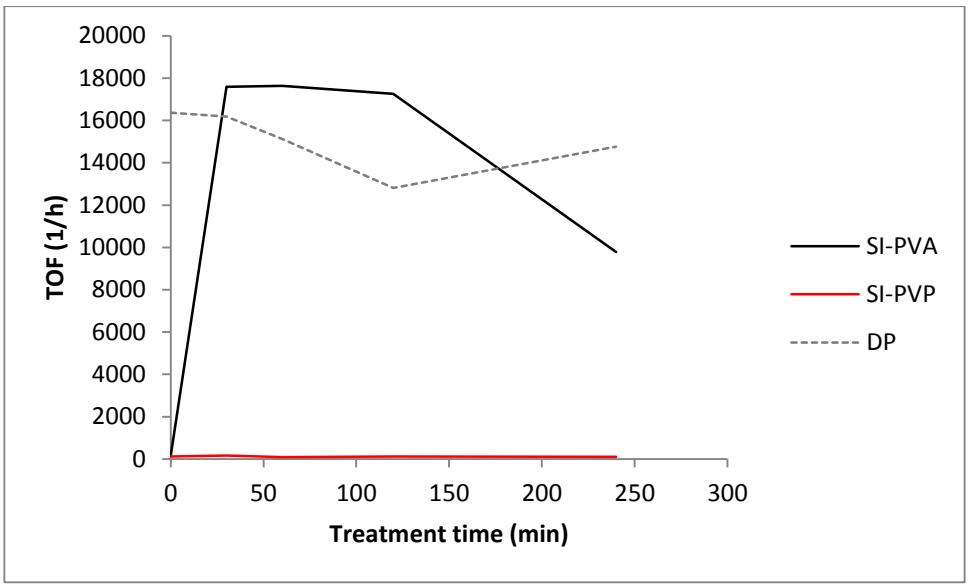

Figure 26: TOF as a function of the treatment time (GHSV=12000, catalyst mass 35 mg, tretment performed at 90 °C).

Data obtained for SI-PVA show the same trend reported by Hutchings and co-workers.[83] DP has been used to see how the treatment influences the supported Au-nanoparticles in their naked form. This catalyst showed a slight deactivation upon treatment. Treatment of the SI-PVP proved not to be effective. Among the causes that could determine the low efficiency of the water treatment on the PVP-stabilized catalyst there is the higher degree of interaction between this polymer and the gold nanoparticle, that could be justified by the 'softer', i.e. more polarizable, behaviour of the nitrogen lone pair, that determines its higher affinity with gold.

TEM data could confirm the shape and size change of the metal upon treatment. The higher stability of the SI-PVA at low treatment time could be justified by an enhanced stability of its particles compared with the DP catalyst, that could be due

to the presence of residual polymer that still exerts its capping agent function, while at the same time it allows the reactants to diffuse to the active site.

Attempts to remove PVP with other *solvents*

The same treatment was performed on SI-PVP catalyst at 90 °C using different solvents. When the boiling point of the solvent was lower than 90 °C the treatment was performed in reflux condition. Different polar solvents were chosen in order to cover a wide range of polarities. Data are reported in the following table (Table 8), along with the dielectric constant of the solvent employed.

Table 8: CO conversion data for solvent treatment on SI-PVP catalyst. GHSV=12000

Catalyst	ε (25 °C)[122]	Conversion %
Not refluxed		≈1 %
2 h refluxed, water pH7	80.4	<0.5 %
2 h refluxed, water pH13 (NaOH)		2.5 %
2 h reflux pH10 (NH3)		4 %
2 h refluxed, water pH1 (H2SO4)		1.7 %
2 h refluxed, isopropanol	18.2	1.3 %
2 h refluxed, acetone	20.7	3.5 %
2 h refluxed, dimethylacetamide	37.7	<0.5 %
2 h refluxed, acetonitrile	37.5	<0.5 %
2 h refluxed, dimethylformamide	38	<0.5 %
2 h refluxed, dimethylsulfoxide	47	<0.5 %
18 h refluxed, H_2SO_4		<1 %
18 h refluxed, NaOH		0 %
18 h refluxed, acetone		1 %
2 h water+acetone		2 %
2 h water+isopropanol		<1 %
2 h water+ethanol		1.5 %
2 h isopropanol+acetone		<1 %

The solvent treatment applied to the SI-PVP catalyst show no improvement on the activity of 1 wt.% Au/TiO_2 catalyst. This is probably due to a stronger interaction between PVP and gold than that between PVA and gold due to the presence of more polarizable “soft” groups, as the lone pair on the aminic nitrogen.

Effect of calcination temperature

The effect of the calcination temperature has been investigated for the three 1 wt.% Au/TiO_2 (SI-PVP, SI-PVA, DP). It was demonstrated that a thermal treatment in air enhances the performances of both PVA-stabilised AuNPs in the oxidation of CO.[83] PVP was removed from PVP-stabilised Pt nanoparticles using calcination at 500 °C, though it was demonstrated that products of its decomposition were still present on the nanoparticles.[99]

Calcination was performed at different temperature and the results for CO oxidation are reported in the following graph (Figure 27).

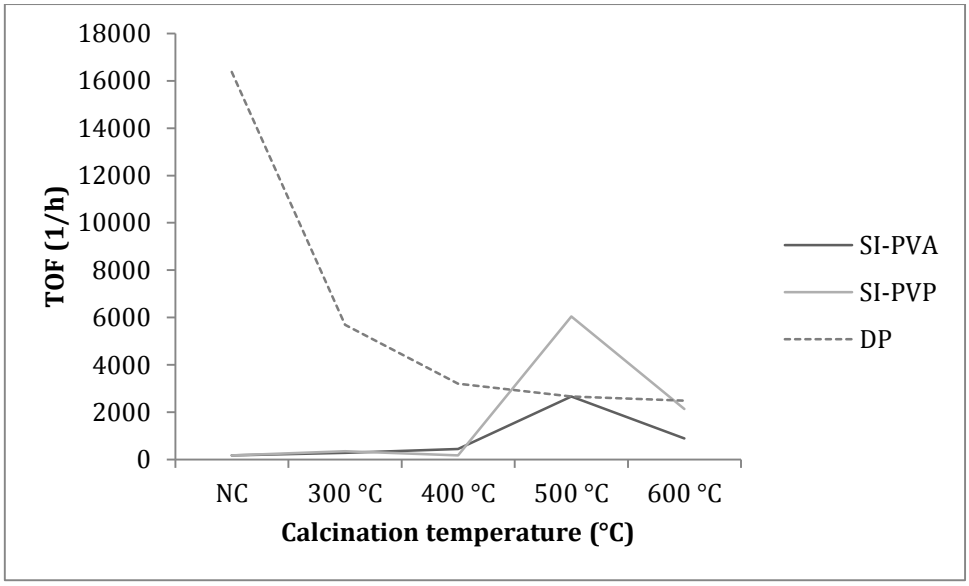

Figure 27: influence of the calcination temperature. NC: not calcined. CO oxidation performed at room temperature, GHSV=12000. Calcination time 4 h, ramp rate 20 °C/min.

The results show that the calcination treatment is partially effective in activating the 1 wt.% Au/TiO_2 catalyst for CO oxidation. In the case of polymer-stabilized catalysts, the minimum temperature for the decomposition of the stabilizing agent is 500 °C. The value obtained at 500 °C has been confirmed by three repetition of the experiments yielding an error below 5%. DP catalysts has been tested as a comparison. It is well known that increasing the calcination temperature of Au/TiO_2 lead to an increase in particle size, leading to a lower amount of active sites and to inactive gold particles.[107,123] It is interesting to note that the SI-PVP catalysts showed higher activity when calcined at 500 °C than the DP one. This is possibly due two

factors, the first being the higher decomposition temperature of PVP, i.e. an increased stabilising effect of the metal particles, and the second the presence of different decomposition products on the metal, leading to a higher degree of poisoning in the case of the PVA stabilised catalyst.[99,124]

DRIFT spectra of the catalyst

Spectra were recorded for the catalyst before and after treatment (Figure 28, Figure 29, Figure 30).

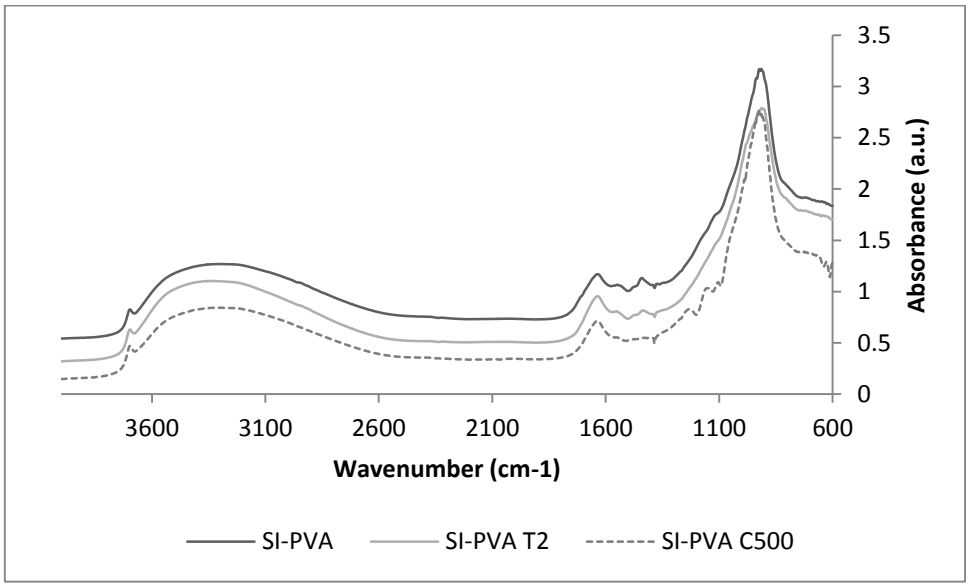

Figure 28: Spectra of the SI-PVA catalyst before (SI-PVA) and after: treatment in 90 °C water, 2 h (SI-PVA T2); calcination at 500 °C for 4 h (SI-PVA C500).

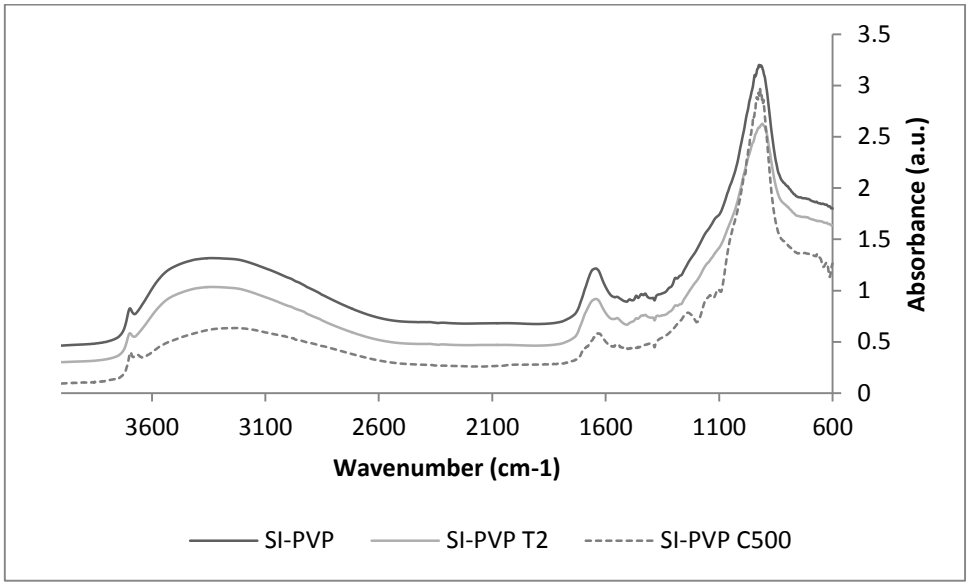

Figure 29: Spectra of the SI-PVP catalyst before (SI-PVP) and after: treatment in 90 °C water, 2 h (SI-PVP T2); calcination at 500 °C for 4 h (SI-PVP C500)

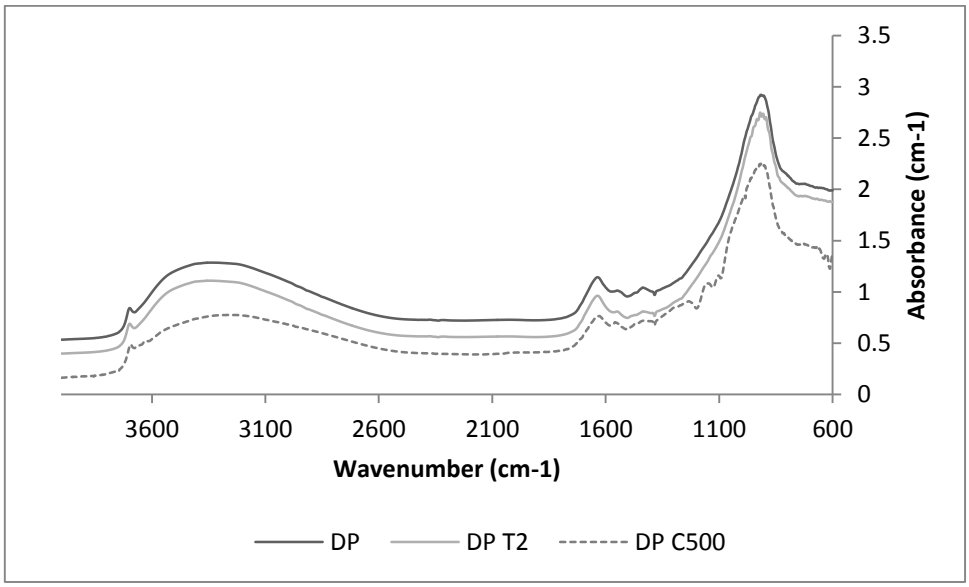

Figure 30: Spectra of the DP catalyst before (DP) and after: treatment in 90 °C water, 2 h (DP T2); calcination at 500 °C for 4 h (DP C500).

From these spectra it is possible to note that it is very difficult to detect bands attributed to PVA or PVP in the pristine sol-immobilization catalysts. Nevertheless it is possible to obtain information about how the treatment in water or the calcination modifies the catalysts. The intensity of the broad band associated to O-H stretching and located between 3000 and 3600 cm^{-1} is decreased by the calcination, indicating, as expected, a diminishment of the functionalities associated with the

presence of adsorbed water on the support. This is confirmed by a decrease in the intensity of the bending mode of adsorbed water at 1600 cm^{-1}. The mechanism of CO oxidation on gold catalysts is not well understood and the literature reports different possibilities.[125] It is nevertheless clear that the presence of water in the gas stream and on the surface of the catalyst plays an important role and influences heavily the performances of the system.[126,127] In the case of the calcined catalysts this factor could play a role in determining the activity, along with possible modification of the metal nanoparticles and the degradation of the polymer in the case of sol-immobilized catalysts.

The DRIFT spectra confirm that no major modification of the support happen upon treatment with 90 °C water or calcination at 500 °C. This technique could not give information about the status of the gold particles, that could be obtained by electron microscopy or through the analysis of spectroscopic features associated with the metal nanoparticle, as for example the surface plasmon resonance (SPR) band.

Reflectance UV-vis spectra of the catalysts

Reflectance UV-vs spectra for the three catalysts are reported in the 500 to 600 nm region, where the SPR band of gold supported on titania is present (Figure 31, Figure 32, Figure 33). Spectra were recorded in nitrogen.

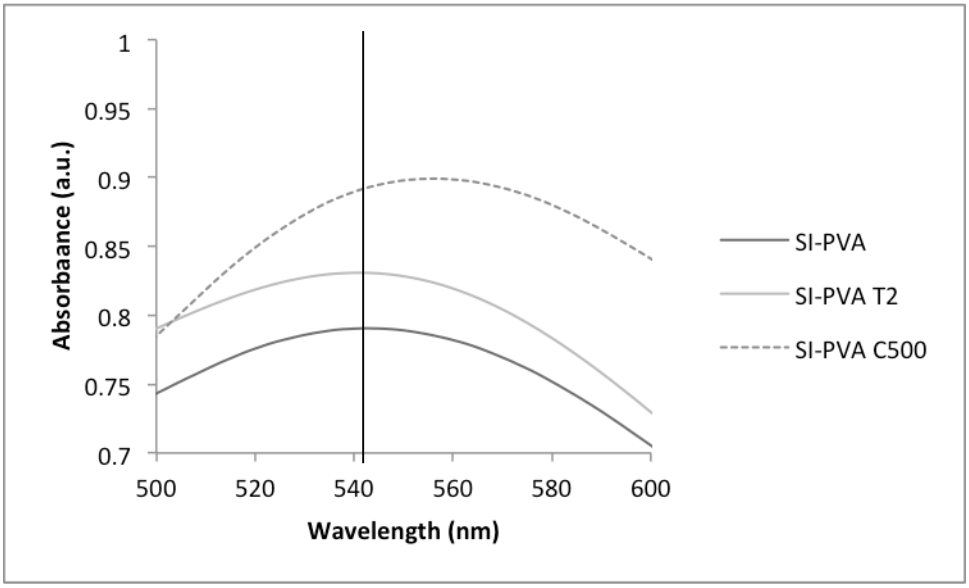

Figure 31: diffuse reflectance UV-vis spectra of the PVA catalyst before and after: treatment in 90 °C water, 2 h (PVA T2); calcination at 500 °C for 4 h (DP C500).

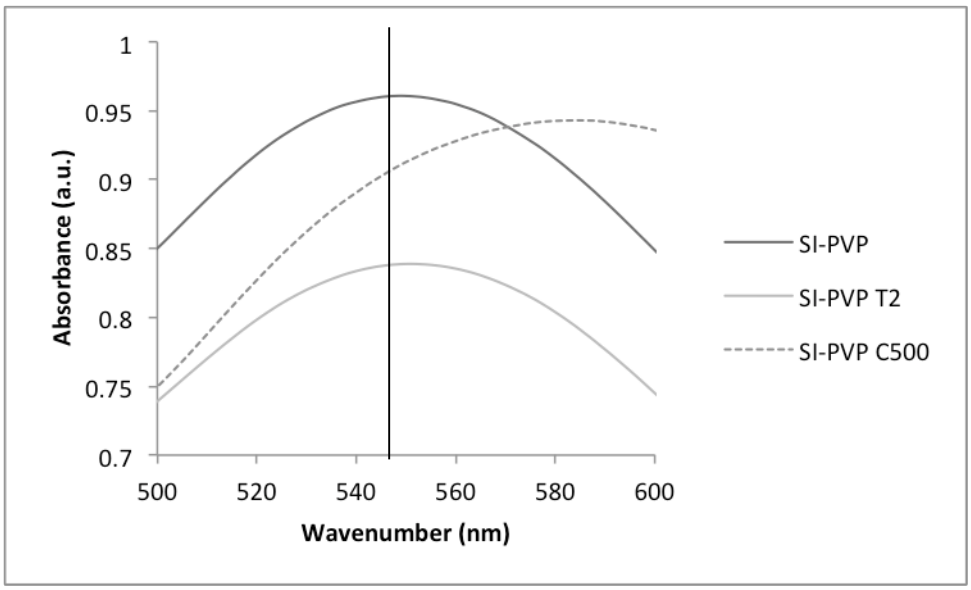

Figure 32: diffuse reflectance UV-vis spectra of the PVP catalyst before and after: treatment in 90 °C water, 2 h (PVP T500); calcination at 500 °C for 4 h (PVP C500).

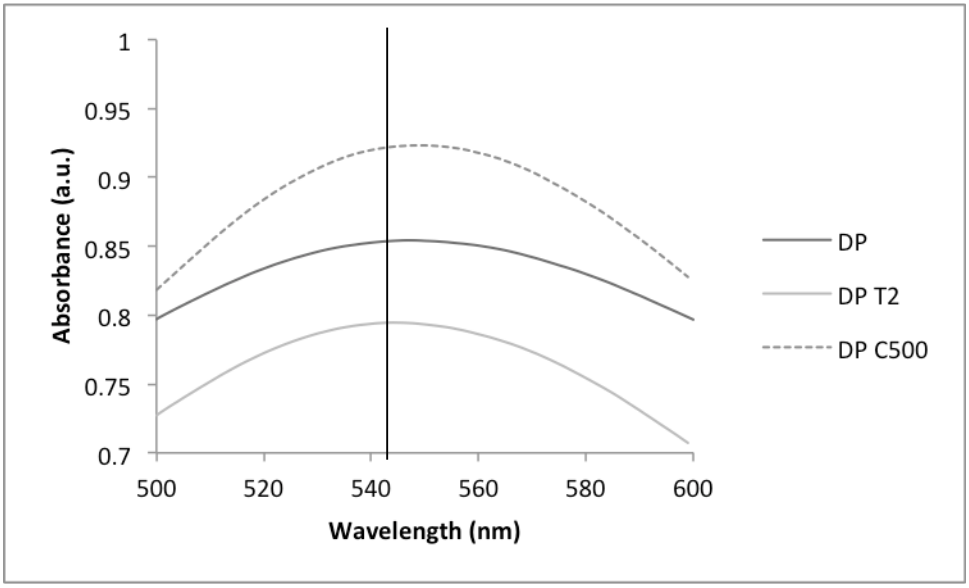

Figure 33: diffuse reflectance UV-vis spectra of the DP catalyst before and after: treatment in 90 °C water, 2 h (DP T2); calcination at 500 °C for 4 h (DP C500).

The plasmon band position arises from the interaction of an electromagnetic wave whose frequency matches that of the surface electrons. As discussed in the introduction its position is influenced by many parameters as polarization of the metal, adsorption of molecules, size and shape of the metal nanoparticles.[112] In this case, as all the spectra are recorded in nitrogen after 15 minutes purge, it is plausible to assume that what influences the most the plasmon resonance frequency is the size and shape of the particle, a change in the adsorption of the polymer (for SI-PVA and SI-PVP) and a marginal effect could be due to a anodic polarization in the case of the calcined samples. It is known that both sol-immobilization and deposition precipitation techniques provide particles with a low aspect ratio and with similar particle size distribution.[83,128-130] Furthermore, the data obtained for the DP catalyst indicate that the electronic properties do not undergo a change upon calcination at 500 °C, probably because equilibrium was already reached upon calcination at 300 °C.

Previous data reported by Hutchings and co-workers, confirmed by the catalytic data reported above, confirms that PVA is removed from the SI-PVA catalyst with a mild treatment in water and that possibly PVP is bound more strongly on the SI-PVP and is not removed.[83] It is possible to note that the position of the plasmon band for the

catalysts treated in water is not modified after the treatment for all the three catalysts tested, hence indicating that the removal of the PVA does not modify the SPR and that the size of the particles is not modified in any case by this treatment.

On the contrary, the UV-vis spectroscopic data for the SPR band of titania supported gold nanoparticles in the case of the calcined catalysts show an evident red shift, that is associated with an increase in the particle size.[116]

Both the information obtained from DRIFT and UV-vis spectroscopy, indicating that a treatment in 90 °C water influences less the morphology of the catalyst than a calcination at 500 °C will be confirmed by future TEM measurements.

CO as a probe molecule: a DRIFT study

The vibrational study of a probe molecule adsorbing on a metal nanoparticle constitute an interesting way of analysing the metal sites that are present and a cheaper alternative to more expensive and time consuming methods (XPS, XANES, XAFS).

The following figure reports the behaviour of the stretching of CO in its adsorption on the not treated catalyst (Figure 34).

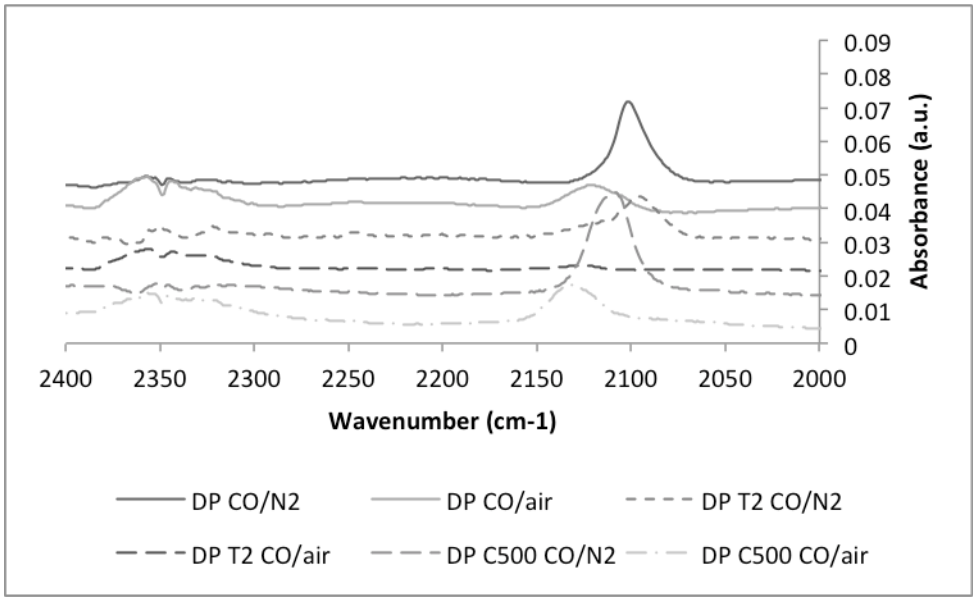

Figure 34: DRIFT for CO adsorbed on DP 1 wt.% Au/TiO_2 before and after treatment.

The position of the linearly adsorbed CO (2100 to 2130 cm^{-1}) changes both upon treatment and upon the different atmosphere the measurement is performed into. Switching the carrier gas from nitrogen to air causes a blue shift of the adsorbed CO band of about 20 cm^{-1} for all the catalysts tested. As discussed in the introduction, this shift could be attributed to both a lower CO coverage, due to the proceeding oxidation reaction, and to the general electron withdrawing effect of the highly electronegative oxygen, that generates partially charged $Au^{\delta+}$ sites.

Comparison of the spectra obtained in nitrogen for the three catalysts

With respect to modification on the rest of the DRIFT spectra, modification induced by the adsorption of CO both in nitrogen and in air could be observed in Figure 35.

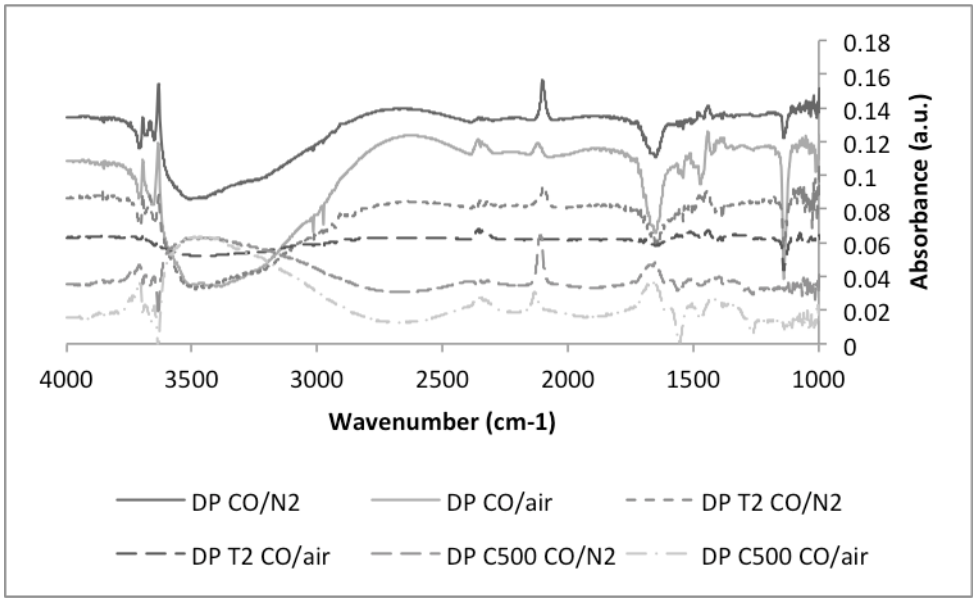

Figure 35: absorbance DRIFT for CO adsorbed on DP 1 wt.% Au/TiO_2 before and after treatment.

In the hydroxyl stretching region it is possible to observe a decrease in the hydrogen bonded OH region for both the untreated and the treated catalysts, while the one calcined at 500 °C shows an increase. These trends are reflected by the OH bending band located at 1600 cm^{-1} and are due to a change in the amount of the water adsorbed on the catalyst. In particular, the decrease in the first two cases could be due to a removal of water by the carrier gas or by a competitive adsorption of CO on the surface, while the second cause is less probable because the band at 2184 cm^{-1}, attributed CO adsorbed on Ti^{4+} sites, is not present.[131] Nevertheless this particular

band has been observed in well-dried catalysts, while in this case catalysts have not been pretreated.

In 0 the DRIFT spectra of the catalysts were shown and the calcined ones showed a lower degree of adsorbed water, especially in the case of SI-PVP and DP. This factor, along with the fact that humidity was not controlled in the gases used for the analyses, could explain why only in the case of calcined DP catalyst it is possible to note an increase of adsorbed water. The calcined SI-PVP does not show any particular modification in the adsorbed water region.

The following figures show the adsorbed CO and the CO_2 region for the SI-PVA (Figure 36) and SI-PVP catalysts (Figure 37).

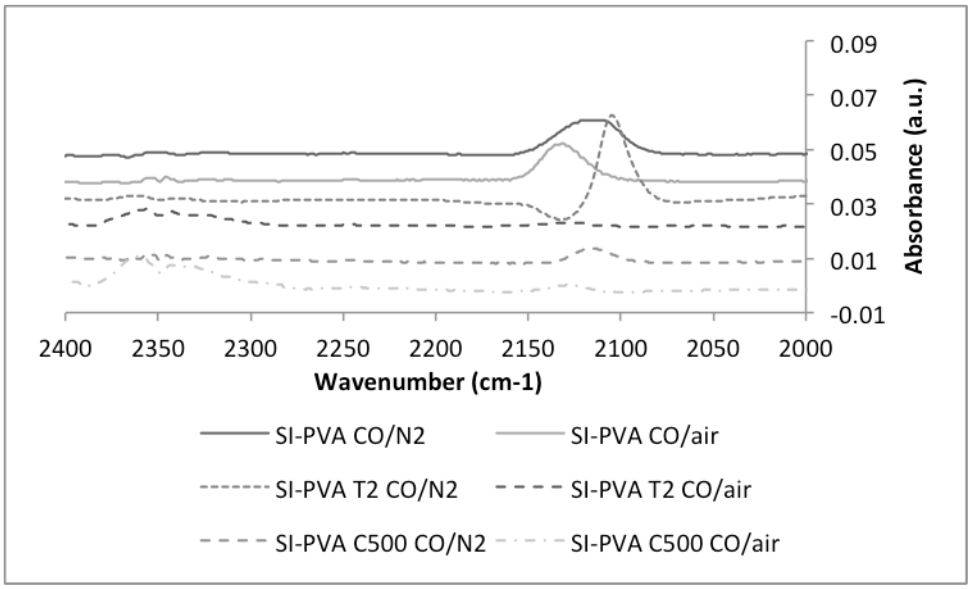

Figure 36: DRIFT for CO adsorbed on the PVA-stabilised 1 wt.% Au/TiO_2 before and after treatment.

While showing no activity for CO oxidation it is interesting to note that the SI-PVA shows the typical band of adsorbed CO even before undergoing any treatment. This is possibly due to the fact that the gold surface is not completely covered by the polymer, and that CO could reach the surface even though an hindrance is exerted, as demonstrated by lower values of activity in the CO oxidation reaction and by the fact that the band for adsorbed CO is located at higher wavenumber (2116 cm^{-1}). This last information indicates a low coverage of the metal surface, i.e. a smaller

active surface. In agreement with what observed for the DP catalyst, changing the carrier gas from nitrogen to oxygen results in a shift of the CO band.

The water treatment of the SI-PVA catalyst results in a clear and sharp CO band that is located at lower wavenumbers (2106 cm^{-1}). This indicates a higher coverage of the surface, that means that the treatment has been successful and most of the surface is available for CO adsorption and oxidation when in the presence of oxygen. In the latter case, high reaction rate could explain depletion of the amount of adsorbed CO and therefore a low intensity of the band associated.

Calcination of the SI-PVA catalyst shows a less intense band slightly blue shifted (2215 cm^{-1}).

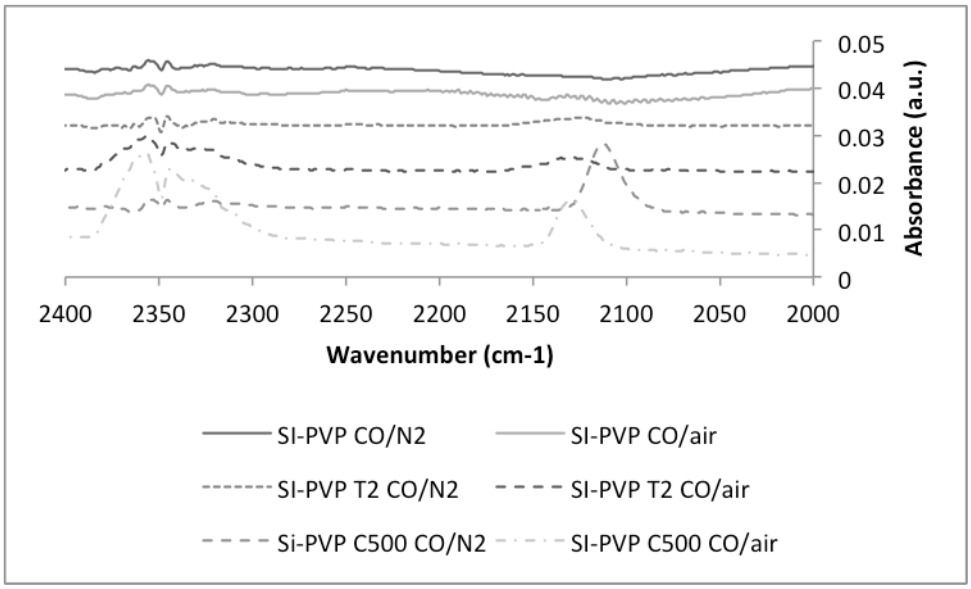

Figure 37: DRIFT for CO adsorbed on the PVP-stabilized 1 wt.% Au/TiO_2 before and after treatment.

SI-PVP catalyst does not show any band of adsorbed CO in the case of the not treated catalyst. The coverage of the surface by PVP seems more complete, and that is possibly due to the stronger polymer-gold interaction. The treatment in water does not influence the layer of polymer on the surface that still prevents CO adsorption. This is in good agreement with the catalytic data.

The only treatment that modifies the adsorption properties of the SI-PVP catalyst is the calcination. CO binds to surface of gold showing a band located at 2113 cm^{-1} and that shifts when oxygen is added to the system.

It is possible to correlate the coverage of the Au particle by CO with the catalytic data, as reported in Figure 38.

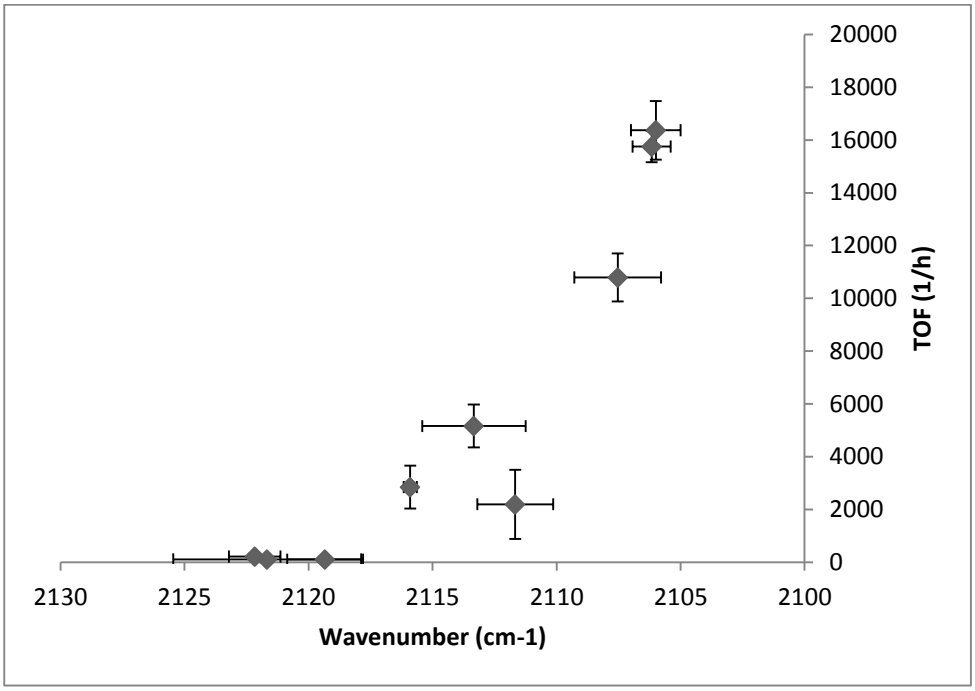

Figure 38: TOF vs. position of the adsorbed CO-band.

Figure 38 shows that only the catalysts where the adsorbed CO band is present at wavenumbers lower than 2115 cm^{-1} show activity in the oxidation of CO. In particular, the activity higher when the position of the band is red shifted. According to the results reported by Boccuzzi et al. this trend could be explained by the different coverage only in the 2102-2115 cm^{-1} region (13 cm^{-1}) shift, while more blue shifted bands are to be attributed to partially positive $Au^{\delta+}$ sites.[107] Electron donation from the CO antibonding orbital to the metal results in increased bond order and therefore higher vibrational frequency. Regarding these kind of sites, it has been reported that they are present in catalysts that have very low activity for CO oxidation.[110,132]

The test proposed confirms the adsorption event analysing a probe molecule. Further information are obtained on the modifications of the titania support, but none are obtained directly about the gold nanoparticle. To gain these evidences UV-vis spectroscopy has been used to analyse the plasmon band of Au nanoparticles.

CO as a probe molecule: a UV-vis study

Spectra were recorded for the DP catalyst to observe the position of the plasmon band upon in-situ addition of carbon monoxide. The resulting spectra are reported in Figure 39 for the untreated sample.

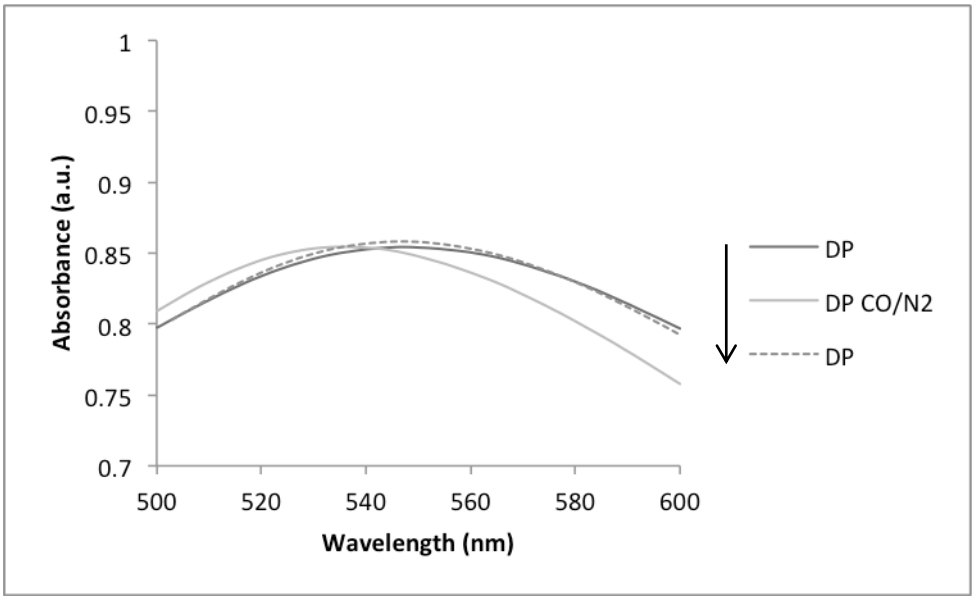

Figure 39: Spectra of the gold SPR band for the DP untreated catalyst in nitrogen, 1 % CO/N_2 and nitrogen.

A blue shift took place upon addition of CO, which showed good reversibility. This is similar to what observed by Sirinakis et al. on Au/YSZ (yttrium stabilised zirconia), but interestingly the shift was observed at room temperature while the previous paper showed that the shift was measurable above 400 °C.[120]

The measurements of the plasmon band position in the presence of oxygen are reported in Figure 40 for the same catalyst.

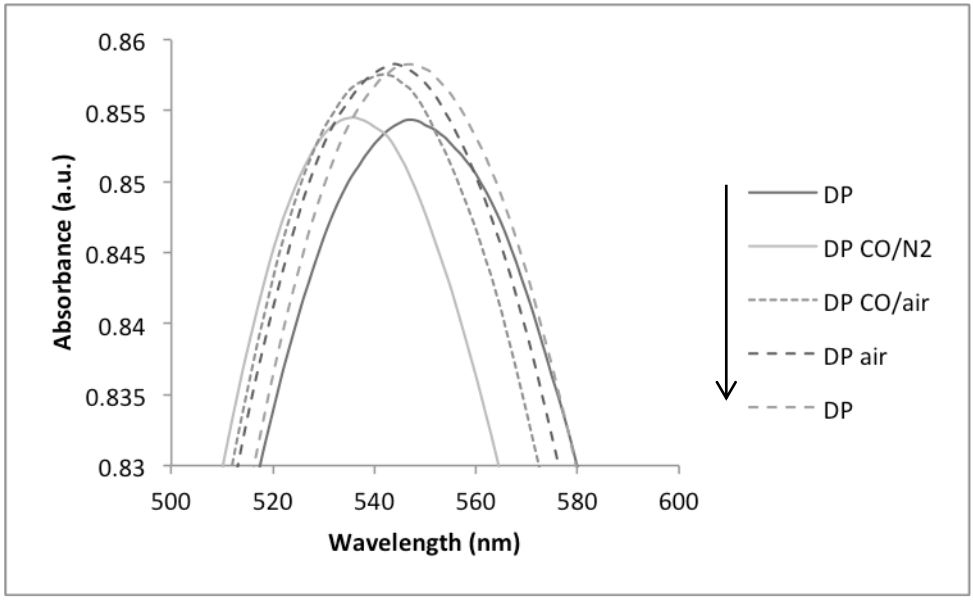

Figure 40: Spectra of the gold SPR band for the DP untreated catalyst in nitrogen, 1 % CO/N_2, 1 % CO/air and nitrogen.

These spectra were recorded for all the three untreated catalysts, the ones treated in water and the calcined ones. For the sake of simplicity only the SPR band spectra of SI-PVA before and after the treatment in water is reported (Figure 41 and Figure 42).

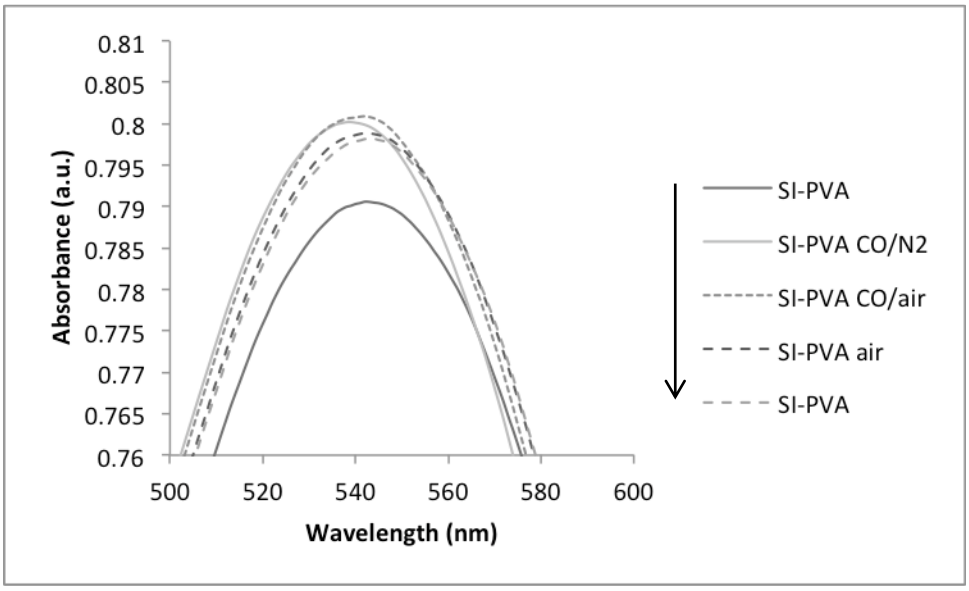

Figure 41: Spectra of the gold SPR band for the PVA untreated catalyst in nitrogen, 1 % CO/N_2, 1 % CO/air and nitrogen.

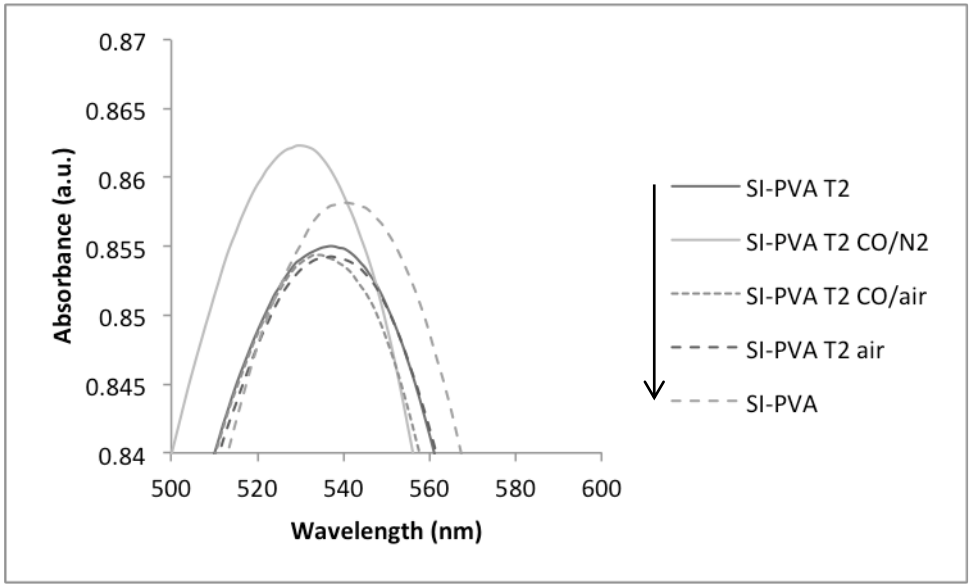

Figure 42: Spectra of the gold SPR band for the PVA catalyst treated in 90 °C water 2 h in nitrogen, 1 % CO/N_2, 1 % CO/air and nitrogen.

The plasmon shift induced by the addition of CO is much more enhanced in the case of the treated catalyst (8 nm vs. 3 nm). It is possible to say that in the case of the treated catalyst there is the possibility for the CO molecule to reach the metal surface, beacause the polymer has been removed or displaced by the treatment.

It is possible to correlate the plasmon shift that is observed in inert atmosphere upon addition of CO with the activity of the catalyst for the CO oxidation reaction at room temperature (Figure 43).

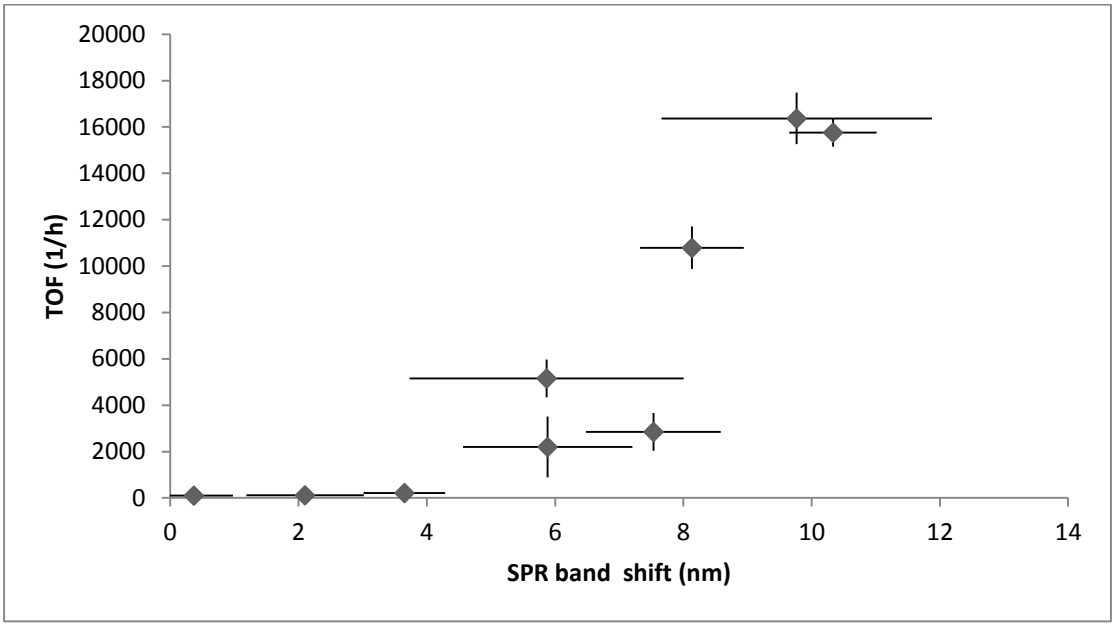

Figure 43: TOF as a function of the observed plasmon shift between N_2 and CO/N_2.

The data shown in Figure 43 show that a relation between the shift of the plasmon band and the activity in the oxidation of CO of 1 wt.% Au/TiO_2 exists. Hypotheses about the causes of this shift are an injection of charge into the nanoparticle by carbon monoxide or a change in the dielectric constant and of the refractive index of the nanoparticle's environment.[118,120] Both these hypotheses are explained in this specific case by an enhanced accessibility of the metal surface that is reached through a treatment in water in the case of the SI-PVA catalyst, and is partially achieved through calcination of the polymer stabilised samples.

2.4. Conclusion

The work performed on sol-immobilization Au/TiO_2 catalysts showed that the removal of PVP from the surface of gold nanoparticles is a more difficult process than the removal of PVA. The simple reflux treatments performed were not effective, though a wide array of solvents were tested.

Nevertheless, the possibility of monitoring the presence of hindrance on the metal surface was shown by means of UV-vis and DRIFT spectroscopies using CO as a probe molecule.

DRIFT spectroscopy allowed seeing no change in the spectra of catalysts with or without a polymer but the band of the CO stretching was observed upon adsorption to the gold surface. When the adsorption was hindered by the presence of PVA or PVP this band was shifted to higher wavenumbers.

Reflectance UV-vis spectroscopy was used to monitor the position of the plasmon band typical of gold nanoparticles. It was shown that this band blue shifts upon adsorption of CO. In the presence of a capping agent this shift is much more limited.

These methods allows for a simple evaluation of the coverage of the gold surface. As a monotonous relationship was shown between the band shift and the catalytic activity, further studies could be performed to make a calibration using known amount of adsorbate in order to have the possibility of predicting through spectroscopic analyses the accessibility of the surface.

3. References

(1) Lange, J. P. *Biofuels, Bioproducts and Biorefining* **2007**, *1*, 39.

(2) Klass, D. L. *Biomass for renewable energy, fuels, and chemicals*; Academic press, 1998.

(3) Farrell, A. E.; Plevin, R. J.; Turner, B. T.; Jones, A. D.; O'hare, M.; Kammen, D. M. *Science* **2006**, *311*, 506.

(4) Hammerschlag, R. *Environmental Science & Technology* **2006**, *40*, 1744.

(5) Antal, M. J. *Advances in solar energy* **1983**, *11*, 111.

(6) Huber, G. W.; Iborra, S.; Corma, A. *Chemical reviews* **2006**, *106*, 4044.

(7) Bozell, J. J.; Moens, L.; Elliott, D.; Wang, Y.; Neuenscwander, G.; Fitzpatrick, S.; Bilski, R.; Jarnefeld, J. *Resources, conservation and recycling* **2000**, *28*, 227.

(8) Kamm, B.; Kamm, M.; Schmidt, M.; Hirth, T.; Schulze, M. *Biorefineries-Industrial Processes and Products: Status Quo and future Directions* **2008**, 97.

(9) Timokhin, B. V.; Baransky, V. A.; Eliseeva, G. D. *Russian chemical reviews* **1999**, *68*, 73.

(10) Werpy, T.; Petersen, G.; Aden, A.; Bozell, J.; Holladay, J.; White, J.; Manheim, A.; Eliot, D.; Lasure, L.; Jones, S. *Top Value Added Chemicals From Biomass. Volume 1-Results of Screening for Potential Candidates From Sugars and Synthesis Gas*, DTIC Document, 2004.

(11) Horváth, I. T.; Mehdi, H.; Fábos, V.; Boda, L.; Mika, L. T. *Green Chem.* **2007**, *10*, 238.

(12) Wolff, L. *Justus Liebigs Annalen der Chemie* **1881**, *208*, 104.

(13) Losanitsch, M. *Monatshefte für Chemie/Chemical Monthly* **1914**, *35*, 307.

(14) Schuette, H.; Sah, P. P. *Journal of the American Chemical Society* **1926**, *48*, 3163.

(15) Sabatier, P.; Mailhe, A. *Ann. Chim. Phys.* **1909**, *16*, 70.

(16) Schuette, H.; Thomas, R. W. *Journal of the American Chemical Society* **1930**, *52*, 3010.

(17) Brunner, E. *Journal of Chemical & Engineering Data* **1985**, *30*, 269.

(18) Kyrides, L. P.; Google Patents: 1945.

(19) Christian Jr, R. V.; Brown, H. D.; Hixon, R. *Journal of the American Chemical Society* **1947**, *69*, 1961.

(20) Dunlop, A. P.; Google Patents: 1957.

(21) Gröger, M. *Zeitschrift für anorganische Chemie* **1908**, *58*, 412.

(22) Gröger, M. *Zeitschrift für anorganische Chemie* **1912**, *76*, 30.

(23) Adkins, H.; Connor, R. *Journal of the American Chemical Society* **1931**, *53*, 1091.

(24) Adkins, H. *Reactions of hydrogen with organic compounds over copper-chromium oxide and nickel catalysts*; University of Wisconsin Press Madison, WI, 1937.

(25) Adkins, H.; Google Patents: 1937.

(26) Adkins, H.; Coonradt, H. L. *Journal of the American Chemical Society* **1941**, *63*, 1563.

(27) Adkins, H.; Burgoyne, E. E.; Schneider, H. J. *Journal of the American Chemical Society* **1950**, *72*, 2626.

(28) Prince, E. *Acta Crystallographica* **1957**, *10*, 554.

(29) Stroupe, J. D. *Journal of the American Chemical Society* **1949**, *71*, 569.

(30) Whipple, E.; Wold, A. *Journal of Inorganic and Nuclear Chemistry* **1962**, *24*, 23.

(31) Broadbent, H. S.; CAMPBELL, G. C.; BARTLEY, W. J.; JOHNSON, J. H. *The Journal of Organic Chemistry* **1959**, *24*, 1847.

(32) Broadbent, H. S.; Selin, T. G. *The Journal of Organic Chemistry* **1963**, *28*, 2343.

(33) Manzer, L. E.; Google Patents: 2003.

(34) Kluson, P.; Cerveny, L. *Applied Catalysis A: General* **1995**, *128*, 13.

(35) Osakada, K.; Ikariya, T.; Yoshikawa, S. *Journal of organometallic chemistry* **1982**, *231*, 79.

(36) Bullock, R. M.; Schlaf, M.; Hauptman, E. M.; Google Patents: 2002.

(37) Starodubtseva, E.; Turova, O.; Vinogradov, M.; Gorshkova, L.; Ferapontov, V. *Russian chemical bulletin* **2005**, *54*, 2374.

(38) Elliott, D. C.; Frye, J. G.; Google Patents: 1999.

(39) MANZER, L.; HUTCHENSON, K.; WO Patent 2,004,113,315: 2004.

(40) Bourne, R. A.; Stevens, J. G.; Ke, J.; Poliakoff, M. *Chemical Communications* **2007**, 4632.

(41) Lazzaroni, M. J.; Bush, D.; Jones, R.; Hallett, J. P.; Liotta, C. L.; Eckert, C. A. *Fluid phase equilibria* **2004**, *224*, 143.

(42) Yan, Z.; Lin, L.; Liu, S. *Energy & Fuels* **2009**, *23*, 3853.

(43) Leardi, R. *Analytica chimica acta* **2009**, *652*, 161.

(44) Serrano-Ruiz, J. C.; Wang, D.; Dumesic, J. A. *Green Chemistry* **2010**, *12*, 574.

(45) Galletti, A. M. R.; Antonetti, C.; De Luise, V.; Martinelli, M. *Green Chemistry* **2012**, *14*, 688.

(46) Upare, P. P.; Lee, J. M.; Hwang, D. W.; Halligudi, S. B.; Hwang, Y. K.; Chang, J. S. *Journal of Industrial and Engineering Chemistry* **2011**, *17*, 287.

(47) Ortiz-Cervantes, C.; García, J. J. *Inorganica Chimica Acta*.

(48) Wettstein, S. G.; Bond, J. Q.; Alonso, D. M.; Pham, H. N.; Datye, A. K.; Dumesic, J. A. *Applied Catalysis B: Environmental* **2012**, *117–118*, 321.

(49) Alonso, D. M.; Wettstein, S. G.; Bond, J. Q.; Root, T. W.; Dumesic, J. A. *ChemSusChem* **2011**, *4*, 1078.

(50) Sen, S. M.; Alonso, D. M.; Wettstein, S. G.; Gurbuz, E. I.; Henao, C. A.; Dumesic, J. A.; Maravelias, C. T. *Energy Environ. Sci.* **2012**, *5*, 9690.

(51) Gürbüz, E. I.; Wettstein, S. G.; Dumesic, J. A. *ChemSusChem* **2012**, *5*, 383.

(52) Primo, A.; Concepción, P.; Corma, A. *Chemical Communications* **2011**, *47*, 3613.

(53) Delhomme, C.; Schaper, L.-A.; Zhang-Presse, M.; Raudaschl-Sieber, G.; Weuster-Botz, D.; Kuehn, F. E. *J. Organomet. Chem.* **2013**, *724*, 297.

(54) Tukacs, J. M.; Kiraly, D.; Stradi, A.; Novodarszki, G.; Eke, Z.; Dibo, G.; Kegl, T.; Mika, L. T. *Green Chemistry* **2012**, *14*, 2057.

(55) Yu, L.; Du, X. L.; Yuan, J.; Liu, Y. M.; Cao, Y.; He, H. Y.; Fan, K. N. *ChemSusChem* **2013**, *6*, 42.

(56) Yan, K.; Liao, J.; Wu, X.; Xie, X. *RSC Advances* **2013**.

(57) Yan, K.; Chen, A. *Energy* **2013**.

(58) Yan, K.; Chen, A. *Fuel* **2013**.

(59) Galletti, A. M. R.; Antonetti, C.; Ribechini, E.; Colombini, M. P.; Di Nasso, N. N. O.; Bonari, E. *Appl. Energy* **2013**, *102*, 157.

(60) Luque, R.; Clark, J. H. *Catalysis Communications* **2010**, *11*, 928.

(61) Di Mondo, D.; Ashok, D.; Waldie, F.; Schrier, N.; Morrison, M.; Schlaf, M. *ACS Catal.* **2011**, *1*, 355.

(62) Castelijns, A. M. C. F.; Janssen, M. C. C.; Vaessen, H. W. L. M.; EP Patent 2,537,840: 2012.

(63) Hengne, A. M.; Rode, C. V. *Green Chemistry* **2012**, *14*, 1064.

(64) Li, W.; Xie, J. H.; Lin, H.; Zhou, Q. L. *Green Chemistry* **2012**, *14*, 2388.

(65) Selva, M.; Gottardo, M.; Perosa, A. *ACS Sustainable Chemistry & Engineering* **2012**, *1*, 180.

(66) DU, X.; LIU, Y.; WANG, J.; CAO, Y.; FAN, K. *Chinese Journal of Catalysis* **2013**, *34*, 993.

(67) Luo, W.; Deka, U.; Beale, A. M.; van Eck, E. R.; Bruijnincx, P. C.; Weckhuysen, B. M. *Journal of Catalysis* **2013**, *301*, 175.

(68) Pan, T.; Deng, J.; Xu, Q.; Xu, Y.; Guo, Q.; Fu, Y. *Green Chem.* **2013**.

(69) Yan, K.; Lafleur, T.; Wu, G.; Liao, J.; Cheng, C.; Xie, X. *Applied Catalysis A: General* **2013**.

(70) Edwards, J. K.; Solsona, B. E.; Landon, P.; Carley, A. F.; Herzing, A.; Kiely, C. J.; Hutchings, G. J. *Journal of Catalysis* **2005**, *236*, 69.

(71) Enache, D. I.; Edwards, J. K.; Landon, P.; Solsona-Espriu, B.; Carley, A. F.; Herzing, A. A.; Watanabe, M.; Kiely, C. J.; Knight, D. W.; Hutchings, G. J. *Science* **2006**, *311*, 362.

(72) Okamoto, H.; Massalski, T. *Journal of Phase Equilibria* **1984**, *5*, 388.

(73) ; Johnson Matthey: Johnson Matthey Website.

(74) Rossetti, I.; Pernicone, N.; Forni, L. *Applied Catalysis A: General* **2003**, *248*, 97.

(75) Oliviero, L.; Barbier, J.; Duprez, D.; Guerrero-Ruiz, A.; Bachiller-Baeza, B.; Rodrıguez-Ramos, I. *Applied Catalysis B: Environmental* **2000**, *25*, 267.

(76) Karakaya, I.; Thompson, W. *Journal of Phase Equilibria* **1986**, *7*, 365.

(77) Swartzendruber, L.; Sundman, B. *Journal of Phase Equilibria* **1983**, *4*, 155.

(78) Charles, J.; Kuntz, J. J.; Gachon, J. C.; Perring, L. *Journal of Phase Equilibria* **1999**, *20*, 573.

(79) Venkatraman, M.; Neumann, J. *Journal of Phase Equilibria* **1987**, *8*, 109.

(80) Nash, P. *Journal of Phase Equilibria* **1986**, *7*, 130.

(81) Wang, J.; Wang, Y.; Xie, S.; Qiao, M.; Li, H.; Fan, K. *Applied Catalysis A: General* **2004**, *272*, 29.

(82) Kabbabi, A.; Faure, R.; Durand, R.; Beden, B.; Hahn, F.; Leger, J.-M.; Lamy, C. *Journal of Electroanalytical Chemistry* **1998**, *444*, 41.

(83) Lopez-Sanchez, J. A.; Dimitratos, N.; Hammond, C.; Brett, G. L.; Kesavan, L.; White, S.; Miedziak, P.; Tiruvalam, R.; Jenkins, R. L.; Carley, A. F.; Knight, D.; Kiely, C. J.; Hutchings, G. J. *Nat Chem* **2011**, *3*, 551.

(84) Niu, Z.; Li, Y. *Chemistry of Materials* **2013**.

(85) Blavo, S. O.; Qayyum, E.; Baldyga, L. M.; Castillo, V. A.; Sanchez, M. D.; Warrington, K.; Barakat, M. A.; Kuhn, J. N. *Topics in Catalysis* **2012**, 1.

(86) Hengne, A. M.; Biradar, N. S.; Rode, C. V. *Catalysis letters* **2012**, *142*, 779.

(87) Bond, G.; Sermon, P. *Gold Bulletin* **1973**, *6*, 102.

(88) Haruta, M.; Kobayashi, T.; Sano, H.; Yamada, N. *Chemistry Letters* **1987**, 405.

(89) Hutchings, G. *Journal of Catalysis* **1985**, *96*, 292.

(90) Hashmi, A. S. K.; Hutchings, G. J. *Angewandte Chemie International Edition* **2006**, *45*, 7896.

(91) Hayashi, T.; Tanaka, K.; Haruta, M. *Journal of Catalysis* **1998**, *178*, 566.

(92) Prati, L.; Rossi, M. *Journal of catalysis* **1998**, *176*, 552.

(93) Landon, P.; Collier, P. J.; Papworth, A. J.; Kiely, C. J.; Hutchings, G. J. *Chemical Communications* **2002**, 2058.

(94) Lopez-Sanchez, J. A.; Dimitratos, N.; Miedziak, P.; Ntainjua, E.; Edwards, J. K.; Morgan, D.; Carley, A. F.; Tiruvalam, R.; Kiely, C. J.; Hutchings, G. J. *Physical Chemistry Chemical Physics* **2008**, *10*, 1921.

(95) Kahsar, K. R.; Schwartz, D. K.; Medlin, J. W. *ACS Catal.* **2013**, *3*, 2041.

(96) Comotti, M.; Della Pina, C.; Matarrese, R.; Rossi, M. *Angewandte Chemie International Edition* **2004**, *43*, 5812.

(97) Comotti, M.; Della Pina, C.; Falletta, E.; Rossi, M. *Advanced synthesis & catalysis* **2006**, *348*, 313.

(98) Rioux, R.; Song, H.; Grass, M.; Habas, S.; Niesz, K.; Hoefelmeyer, J.; Yang, P.; Somorjai, G. *Topics in Catalysis* **2006**, *39*, 167.

(99) Du, Y.; Yang, P.; Mou, Z.; Hua, N.; Jiang, L. *Journal of applied polymer science* **2006**, *99*, 23.

(100) Aliaga, C.; Park, J. Y.; Yamada, Y.; Lee, H. S.; Tsung, C.-K.; Yang, P.; Somorjai, G. A. *The Journal of Physical Chemistry C* **2009**, *113*, 6150.

(101) Crespo-Quesada, M.; Andanson, J.-M.; Yarulin, A.; Lim, B.; Xia, Y.; Kiwi-Minsker, L. *Langmuir* **2011**, *27*, 7909.

(102) Ansar, S. M.; Ameer, F. S.; Hu, W.; Zou, S.; Pittman Jr, C. U.; Zhang, D. *Nano letters* **2013**, *13*, 1226.

(103) Yates, D. *Journal of Colloid and Interface Science* **1969**, *29*, 194.

(104) Dumas, P.; Tobin, R.; Richards, P. *Journal of Electron Spectroscopy and Related Phenomena* **1986**, *39*, 183.

(105) France, J.; Hollins, P. *Journal of electron spectroscopy and related phenomena* **1993**, *64*, 251.

(106) Boccuzzi, F.; Chiorino, A.; Tsubota, S.; Haruta, M. *The Journal of Physical Chemistry* **1996**, *100*, 3625.

(107) Boccuzzi, F.; Chiorino, A.; Manzoli, M.; Lu, P.; Akita, T.; Ichikawa, S.; Haruta, M. *Journal of catalysis* **2001**, *202*, 256.

(108) Boccuzzi, F.; Tsubota, S.; Haruta, M. *Journal of electron spectroscopy and related phenomena* **1993**, *64*, 241.

(109) Bollinger, M. A.; Vannice, M. A. *Applied Catalysis B: Environmental* **1996**, *8*, 417.

(110) Grunwaldt, J.-D.; Maciejewski, M.; Becker, O. S.; Fabrizioli, P.; Baiker, A. *Journal of Catalysis* **1999**, *186*, 458.

(111) Zeng, S.; Yong, K.-T.; Roy, I.; Dinh, X.-Q.; Yu, X.; Luan, F. *Plasmonics* **2011**, *6*, 491.

(112) Mulvaney, P. *Langmuir* **1996**, *12*, 788.

(113) Homola, J.; Yee, S. S.; Gauglitz, G. *Sensors and Actuators B: Chemical* **1999**, *54*, 3.

(114) Liedberg, B.; Nylander, C.; Lunström, I. *Sensors and actuators* **1983**, *4*, 299.

(115) Willets, K. A.; Van Duyne, R. P. *Annu. Rev. Phys. Chem.* **2007**, *58*, 267.

(116) Eustis, S.; El-Sayed, M. A. *Chemical Society Reviews* **2006**, *35*, 209.

(117) Ando, M.; Kobayashi, T.; Iijima, S.; Haruta, M. *J. Mater. Chem.* **1997**, *7*, 1779.

(118) Ando, M.; Kobayashi, T.; Iijima, S.; Haruta, M. *Sensors and Actuators B: Chemical* **2003**, *96*, 589.

(119) Ando, M.; Kobayashi, T.; Haruta, M. *Catalysis Today* **1997**, *36*, 135.

(120) Sirinakis, G.; Siddique, R.; Manning, I.; Rogers, P. H.; Carpenter, M. A. *The Journal of Physical Chemistry B* **2006**, *110*, 13508.

(121) Steinhauser, G.; Evers, J.; Jakob, S.; Klapötke, T. M.; Oehlinger, G. *Gold Bulletin* **2008**, *41*, 305.

(122) Lide, D. R. *CRC Handbook of Chemistry and Physics 2004-2005: A Ready-Reference Book of Chemical and Physical Data*; CRC press, 2004.

(123) Park, E. D.; Lee, J. S. *Journal of Catalysis* **1999**, *186*, 1.

(124) Guirguis, O. W.; Moselhey, M. T. *Nat Sci* **2012**, *4*, 57.

(125) Bond, G. C.; Thompson, D. T. *Gold Bulletin* **2000**, *33*, 41.

(126) Date, M.; Haruta, M. *Journal of catalysis* **2001**, *201*, 221.

(127) Wang, G. Y.; Zhang, W. X.; Lian, H. L.; Jiang, D. Z.; Wu, T. H. *Applied Catalysis A: General* **2003**, *239*, 1.

(128) Haruta, M. *Catalysis Today* **1997**, *36*, 153.

(129) Haruta, M.; Tsubota, S.; Kobayashi, T.; Kageyama, H.; Genet, M. J.; Delmon, B. *Journal of Catalysis* **1993**, *144*, 175.

(130) Dimitratos, N.; Lopez-Sanchez, J. A.; Morgan, D.; Carley, A.; Prati, L.; Hutchings, G. J. *Catalysis today* **2007**, *122*, 317.

(131) Morterra, C. *J. Chem. Soc., Faraday Trans. 1* **1988**, *84*, 1617.

(132) Daniells, S.; Overweg, A.; Makkee, M.; Moulijn, J. *Journal of Catalysis* **2005**, *230*, 52.